Received: 9 & 24 October, 2012
IOTC-2012-WPTT14-23 Rev_1

UPDATED GROWTH ESTIMATES FOR SKIPJACK, YELLOWFIN AND BIGEYE TUNA IN THE INDIAN OCEAN USING THE MOST RECENT TAG-RECAPTURE AND OTOLITH DATA

J. Paige Eveson[1]
Julien Million[2]
Fany Sardenne[2,3]
Gaël Le Croizier[2]

[1] CSIRO Marine and Atmospheric Research, GPO Box 1538, Hobart, Tasmania 7001, Australia
[2] Indian Ocean Tuna Commission, PO Box 1011, Victoria, Seychelles
[3] Institut de Recherche pour le Dévelopement, UMR 6539 LEMAR (UBO/CNRS/IRD/ Ifremer), BP70, 29280 Plouzané, France

Prepared for the IOTC Working Party on Tropical Tunas, 24-29 October 2012, Grand Baie International Conference Centre, Mauritius

Table of Contents

Abstract

Results from fitting multi-stanza parametric growth models to the most recent mark-recapture data from yellowfin (*Thunnus albacores*), bigeye (*T. obesus*) and skipjack (*Katsuwonus pelamis*) tuna in the Indian Ocean are presented. The models were fit using a maximum likelihood method that models the joint density of release and recapture lengths as a function of age by treating age at tagging as a random variable. The method allows for individual variability in growth by modelling the asymptotic length parameter as a random effect. This method was first applied to the Indian Ocean tagging data from all three species in 2008 (Eveson & Million 2008a,b), and updated for skipjack in 2011 (Eveson 2011). Otolith readings data were also integrated into the models for yellowfin and bigeye since a preliminary investigation of the otolith readings from tag-recaptured fish that were injected with oxytetracycline (OTC) at the time of tagging suggests that daily rings are formed in the otoliths of these species; this does not appear to be the case for skipjack. The updated results continue to support a two-stanza VB growth model for yellowfin and bigeye, and provide stronger evidence that a two-stanza VB model is more appropriate for skipjack as well. Differences in growth between sexes were also found for yellowfin and bigeye, with males growing to a larger size.

Introduction

Growth information for yellowfin (YFT), bigeye (BET) and skipjack (SKJ) tuna in the Indian Ocean is limited and remains a key area of uncertainty in stock assessments for these species (IOTC-2011-WPTT13 2011). Most recent studies suggest that a two-stanza growth curve, with an increase in the rate of growth between juveniles and adults, is most appropriate for YFT and BET, and perhaps SKJ as well, although the evidence for SKJ has not been as clear (e.g., Fonteneau & Gascuel, 2008; Eveson & Million 2008a,b; Hillary et al. 2008; Morize et al., 2008; Dortel et al. 2011). In any case, the exact form and parameterization of the growth curve for each species is still being debated (IOTC-2011-WPTT13 2011).

One of the goals of the Regional Tuna Tagging Project of the Indian Ocean (RTTP-IO) was to provide estimates of growth parameters for tuna in the Indian Ocean. As part of this project, large numbers of YFT, BET and SKJ were tagged between October 2005 and August 2007 by trained technicians. Tagging occurred in the western Indian Ocean, primarily off Tanzania. Details of the RTTP-IO tagging operations can be found in Hallier (2008). Additional tagging has also occurred in the eastern Indian Ocean as part of small-scale tagging operations, including extensive tagging of SKJ and YFT off the Maldives in 2004 and 2007-2009. Collectively, the RTTP-IO and small-scale tagging operations are known as the Indian Ocean Tuna Tagging Programme (IOTTP). In total, over 63 000 YFT, 35 000 BET, and 100 000 SKJ have been tagged since 2004. Recaptures have occurred in the commercial fisheries operating in the Indian Ocean, with returns coming primarily from the purse seine fishery. The low number of returns from other fisheries is partly due to lower catch numbers, particularly of the smaller size classes that were tagged, but probably due to in most-part to non-reporting. To date, the percent of tag returns is approximately 16% for each of the three species.

The change in length of a tagged fish between the time it was released and the time it was recaptured provides useful information for modelling growth. Because the age of a fish at release is unknown, the traditional approach has been to model the incremental change in length of the fish over the time it was at liberty (Fabens 1965; Francis 1988; James 1991). This approach can lead to

biased parameter estimates when individual variability in growth exists (Sainsbury 1980). More recently, maximum likelihood approaches have been developed that model the joint density of the release and recapture lengths as opposed to modelling the length increment (Palmer et al. 1991; Wang et al. 1995; Laslett et al. 2002). In these cases, the age at release is modelled as a random variable. For this report, the method of Laslett et al. (2002), which will be referred to as the LEP (Laslett, Eveson and Polacheck) method, was applied to the tag-recapture data for YFT, BET and SKJ.

Tag-recapture data does not provide information about absolute age, only relative age; therefore auxiliary information is required to anchor the curve to an absolute age axis. As part of the RTTP-IO, a large number of fish were injected at the time of tagging with oxytetracycline (OTC), a chemical that leaves a mark in the otolith of the fish. This chemical tagging allows for validation of ages read directly from the otoliths of recaptured OTC-marked fish. Recently, a number of otoliths sampled from YFT, BET and SKJ caught in the Indian Ocean during the course of the RTTP-IO have been read at the LEMAR laboratory in France; this includes as many of the OTC-marked YFT and BET recaptures as possible (only a few OTC-marked SKJ otoliths were read, as SKJ was deemed lower priority). A preliminary investigation of the OTC-marked otolith readings shows a linear relationship between the number of rings deposited and the number of days between tagging and recapture for YFT and BET. Based on this relationship, the otolith readings were converted to age estimates and included in the growth models for YFT and BET through an additional likelihood component. Results are presented from the integrated tag-recapture and otolith growth models, and consistency between the two data sources is evaluated.

Data

Tag-recapture data

Tag-recapture data obtained as part of the RTTP-IO as well as from the small-scale tagging operations were included in this report[1], provided the releases and recaptures met all screening criteria. Not all data are appropriate for growth analysis since some of the necessary information may be missing or unreliable. Thus, a screening process was applied to the data prior to analysis according to the criteria outlined in Appendix IX of IOTC-2011-WPTT13 (2011)[2]. The number of release-recapture pairs considered appropriate for analysis after screening was: 4404 for YFT; 3086 for BET and 4997 for SKJ. These sample sizes are significantly greater (2-3 times) than were available for the growth analysis conducted in 2008 (Eveson & Million 2008a,b). Sex information exists for some of the larger recaptures of YFT (53 males and 32 females) and BET (38 males and 29 females), which provides important information on sex differences in asymptotic length.

Otolith data

The otolith data considered in this report are from YFT, BET and SKJ samples collected in the Indian Ocean during 2006-2011 and read at the LEMAR laboratory in France (see Dortel et al. 2012 for details). Otoliths were read from tuna that were: 1) tagged as part of the RTTP-IO and OTC-marked, 2) tagged but not OTC-marked, and 3) not tagged. Before the otolith readings could be used for

[1] The version of the tag database available at the time of analysis was dated 2012-07-05.

[2] The final criterion states that tags reported prior to 1April 2007 (prior to recovery teams being placed onboard purse seine vessels calling in port Victoria) should be used with caution as there is uncertainty in the dates and positions of recovery. To be conservative, recaptures prior to this date were omitted from the analysis; however, some sensitivity runs including these data were conducted and the results were not significantly affected.

growth modelling, we needed to establish whether a relationship exists between the number of otolith increments and the age of the fish. This could be done using the OTC-marked samples by comparing the number of increments counted after the OTC mark (denoted by S2) with the number of days the fish was at liberty. Because most samples have multiple reads by one or more readers, we first looked for differences between readers. In our initial investigation we did not find any significant reader effects (see Appendix A, Figure A1), so we averaged across all reads for a sample to get a single estimate for that otolith[3]. We then fit a separate linear regression for each species with mean S2 count as the response variable and days at liberty as the explanatory variable. An almost 1:1 linear relationship was found for YFT and BET, with the counts being slightly smaller on average than the days at liberty (Appendix A, Figures A2 and A3). This suggests that YFT and BET do in fact deposit daily, or almost daily, increments, with the slight negative bias in the counts being due to either biological effects (increments not being formed on a small percent of days) and/or reader effects (increments not getting counted, perhaps when they are too close together to distinguish). Thus, for all the YFT the BET samples (not just OTC-marked ones, but all samples that were read), we estimated a fish's age by averaging over all its total increment counts (Stot), and then adjusting the average using the results of the linear regression (see Appendix A for details). A summary of the resulting YFT and BET direct ageing data available for growth modelling can be found in Appendix A (Table A2; Figure A4). For SKJ, the S2 counts were significantly smaller than the days at liberty, suggesting increments are not deposited daily (Appendix A, Figure A2). Given that the relationship between increment formation and time/age is not well understood for SKJ, the SKJ otolith data were not used in subsequent growth modelling.

Methods

Before fitting growth models to the data, an exploratory analysis was undertaken which included calculating an average growth rate (cm/day) for each fish by dividing the difference between its recapture length and release length by the number of days it was at liberty. The purpose was to look for broad patterns in the data and to help determine an appropriate functional form for the growth curve used for each species.

Based on the exploratory plots, a two-stanza growth model was deemed most appropriate for all three species. In particular, we chose to fit the VB log k growth function (von Bertalanffy with a logistic growth rate parameter) of Laslett et al. (2002). This function can be expressed as

$$l(a) = L_\infty f(a - a_0; \theta)$$

where L_∞ is asymptotic length, $\theta = \{k_1, k_2, \alpha, \beta\}$ and

$$f(a - a_0; \theta) = 1 - \exp(-k_2(a - a_0)) \left\{ \frac{1 + \exp(-\beta(a - a_0 - \alpha))}{1 + \exp(\alpha\beta)} \right\}^{-(k_2 - k_1)/\beta}$$

[3] Subsequent investigation of the data after the growth models had already been fit suggests there are complex reader effects, with S2 counts appearing to be consistent among all readers, but not total (Stot) counts. See Appendix A for more details. How best to deal with reader effects in determining age estimates is an important issue to discuss at the upcoming WPTT meeting.

The parameter a_0 can be thought of as the theoretical age at which a fish would have had length 0 if we were to project its growth curve backwards. This parameter cannot be estimated from tag-recapture data alone, so in order to fully define the growth curve it must be determined from other sources, such as direct age data from otoliths (or other calcified structures).

The equation for the VB log k function represents a change in growth from a VB curve with growth rate parameter k_1 to a VB curve with growth rate parameter k_2, with a smooth transition between the two stages governed by a logistic function. The parameter α governs the age at which the midpoint of the transition occurs, and β governs the rate of the transition (being sharper for larger values).

Tag-recapture likelihood

The VB log k growth model was fit to the tag-recapture data using the LEP method. Details of the method can be found in Laslett et al. (2002). The key feature of this method is that it models the release and recapture lengths as functions of age by treating age at tagging, *A*, as a random variable[4]. *A* is assumed to follow a specified distribution, and the parameters of this distribution are estimated within the model. In applying the LEP method to the three tuna data sets, a lognormal distribution with parameters $\mu_{\log A}$ and $\sigma_{\log A}$ was chosen for *A*. Laslett et al. (2002) showed that the results were fairly robust to the distribution used for *A* so long as it provided a reasonable approximation. Another feature of the LEP method is that it allows for individual variability in growth by modelling the asymptotic length parameter as a random effect. For all species, L_∞ was assumed to follow a normal distribution with mean $\mu_{L\infty}$ and standard deviation $\sigma_{L\infty}$. The model allows for extra variability in length at age on top of the variability in L_∞ through an additive Gaussian error component with mean 0 and standard deviation σ_{tag}, which represents measurement error and/or additional process error.

Residual plots were used to evaluate the fits. Note that to calculate the fitted recapture values (and thus the residuals) for the LEP method requires a realized value of *A* for each fish. A natural approach is to use the mean of the posterior distribution for *A* conditional on the fish's release and recapture lengths. However, as explained in Laslett et al. (2004), this approach yields biased estimates, so we used the approximately conditionally unbiased estimator for *A* proposed in Laslett et al. (2004) instead.

Otolith likelihood

For YFT and BET, the estimated ages from the otoliths along with the lengths of the fish at capture could be included in the growth model through an additional likelihood component. We assumed a Gaussian error structure for length at age, with mean

$$E\{l(a)\} = \mu_{L\infty} f(a - a_0; \theta)$$

and variance

[4] Note that *A* actually represents the age at tagging, a_1, relative to a_0 (i.e., $A = a_1 - a_0$). As noted previously, it is not possible to estimate a_0 from tagging data alone.

$$V\{l(a)\} = (\sigma_{L\infty} f(a - a_0; \theta))^2 + \sigma_{oto}^2$$

where the first component of variance is due to individual variability in L_∞ and the second component is additional measurement/process error component. Thus the likelihood for the otolith data is just the product of Gaussian densities over all fish. While overly simplistic, we input the age estimates to the model as if they were known accurately; statistically rigorous approaches for dealing with errors-in-variables models exist but we did not have time to pursue them for this report. Note that, unlike with the tag-recapture likelihood, the parameters that can be estimated from optimizing the otolith likelihood include a_0.

Because the otolith growth data and tag-recapture growth data are independent, the log likelihoods for the two data sets could be added together and the parameters estimated by minimizing the total negative log likelihood.

Results

Yellowfin

Figure Y1 shows histograms of the release lengths, recapture lengths and times at liberty for recaptured YFT. There are two modes in the release lengths at ~ 48cm and 62cm that possibly correspond to age classes. The mean time at liberty was 478 days and the maximum was 2139 days. Figure Y2 shows the length increment (recapture minus release length) plotted against the number of days at liberty. Two bands can be distinguished in this figure. These correspond to fish from the two modes in the release length distribution. Specifically, the lower band, which represents slower growth, corresponds to fish from the smaller mode. This figure also reveals that a number of length increments are negative, indicating that measurement error can be significant. Figure Y3 shows the average growth rate, calculated as centimetres growth per day, plotted against release length. There is a clear change in growth rates at a length of about 55cm, with smaller fish growing more slowly than larger fish. This lends strong support for a two-stanza growth model. Kolody (2008) suggested that the apparent two-stanza growth might be an artefact of different size-selectivities between the FAD and free-school components of the purse seine fishery (with the latter catching larger fish). However, the same two-stage pattern in growth rates can be seen in the data for fish caught in both components (Figure Y3(b)).

The otolith age and length data available for YFT are shown in Appendix A (Figure A4(a)). These data also seem to support a two-stanza growth model for YFT, with a change in growth occurring around age 2.

Parameter estimates from fitting the VB log k model jointly to the YFT tag-recapture and otolith data can be found in Table Y1. Convergence was difficult to achieve and parameter estimates were sensitive to the starting values, suggesting the likelihood surface may be flat in places and/or contain multiple minima; thus, the results should be considered with some caution. Hillary et al. (2008) found similar convergence issues in fitting flexible growth models to the YFT and BET tagging data. Diagnostic plots are shown in Figure Y4. Figure Y4(a) shows the estimated release ages for all fish, overlaid with the estimated lognormal distribution (note that the age and log normal distribution estimates obtained directly represent age relative to a_0, but the age axis has been shifted by the

estimated value of a_0 so that it represents absolute age). Even though a uni-modal distribution is being assumed, the individual age estimates are still able to capture the bi-modal nature of the release ages suggested by the release lengths. Figure Y4(b) shows the release and recapture lengths plotted against estimated age, along with the mean fitted growth curve. Figure Y4(c) shows the release and recapture length residuals (fitted minus true); a smooth through the points suggests a reasonably good fit. Finally, Figure Y4(d) shows the residuals for the otolith data. There is an obvious lack of fit in length at age for young/small fish (<1.5 years), which is apparent in Figure Y4(b) as well. The otolith data suggest much faster initial growth than the tag-recapture data.

The sample size is so much larger for the tag-recapture data than the otolith data that the otolith data has very little influence on the model fit except to allow a_0 to be estimated. Therefore, for comparison, we refit the model with the otolith likelihood highly weighted (multiplied by a factor of 100) so that it would have more influence than the tag-recapture likelihood. The results are given in Table Y1 and Figure Y5(a-d). In this case initial growth is estimated to be faster (k_1 estimated to be 0.31 instead of 0.20) and, correspondingly, a_0 is estimated to be larger (i.e., closer to zero). Also, the variance in the distribution of L_∞ ($\sigma_{L\infty}$) is estimated to be much greater while the measurement error for the otolith data is estimated to be much smaller; this is because the otolith data show surprisingly low variability in length at age for young ages but huge variability for older ages, which can best be explained by a large $\sigma_{L\infty}$ value. The remaining parameters remain similar to the original fit (keeping in mind that α, which governs the age at which the transition between stages occurs, is relative to a_0, so equates to an absolute age of ~2.2 years in both models). Not surprisingly, the residuals for the tag-recapture data do not look quite as good (Figure Y5(c)), but the residuals for the otolith data are improved (Figure Y5(d)).

Sex information exists for a relatively small number of YFT recaptures (53 males, 32 females), all of which are large fish (ranging from 106 to 160cm) recaptured after being at liberty for several years (average of ~4 yrs) (see Figure Y6). Unfortunately the data with sex information are insufficient for estimating all parameters of the VB log k growth model freely, especially since they contain very little information about growth during the transition between growth stages. However, we were able to fit the model by fixing several parameters. In particular, we chose to fix the parameters governing the age and speed of transition (α and β), the parameters of the release age distribution ($\mu_{\log A}$ and $\sigma_{\log A}$), and a_0 at the maximum likelihood estimates from the joint tag and otolith fit to all data with the otolith data highly weighted (i.e., the values from Table Y1, row 2). The results (Table Y2; Figure Y6) support the hypothesis that, on average, male YFT grow to a larger size than female YFT, with the mean asymptotic length estimate for males being 150cm versus 140cm for females. Interestingly, even the $\mu_{L\infty}$ estimate for females is larger than the estimate obtained using all the (non-sex-specific) data (~130cm in both the models with and without the otolith data weighted).

Based on the asymptotic length estimates for males and females and on maximum lengths found in the catch data for YFT, we refit the VB log k model to the all the tag-recapture and otolith data fixing $\mu_{L\infty}$ at 145cm. We did so with and without weighting the otolith data (Table Y1). The largest effect is that the growth rate parameter for the second stage, k_2, becomes smaller, which is not surprising

since it is negatively correlated with $\mu_{L\infty}$. The negative log likelihoods are significantly larger when $\mu_{L\infty}$ is fixed than when it is estimated freely (>200 units), but a statistically better fit is not always a more biologically realistic one.

A comparison of all the mean VB log k growth curves presented above for YFT is given in Figure Y7.

Bigeye

Figures B1-B3 for BET are analogous to Figures Y1-Y3 for YFT. As with YFT, there appear to be two modes in the release lengths at ~ 48cm and 62cm (Figure B1), although the second mode is much smaller in this case. The recapture lengths are also much smaller on average, and the times at liberty shorter (mean of 345 days, maximum of 2485 days). Two bands in the plot of length increments versus days at liberty are also present for BET (Figure B2) but they are not distinguishable in this figure because they are closer together and masked by the variability. Figure B3, showing the average growth rate versus release length, strongly supports a two-stage growth model for BET as well, with the change from slower to faster growth occurring at a very similar length as YFT (~55cm). For BET, however, the change in growth rate between the two stages is not as extreme.

The otolith age and length data available for BET are shown in Appendix A (Figure A4(b)). Unfortunately, unlike for YFT, there are no age estimates for fish less than 45cm in length and very few estimates for fish over 100cm. Thus, the data contain minimal information about growth for BET, especially the shape of the growth curve; however, they are still useful for anchoring the growth curve to an absolute age axis.

Parameter estimates from fitting the VB log k model jointly to the BET tag-recapture and otolith data can be found in Table B1. The best fit to the tag-recapture data suggests growth for young fish is very slow, almost flat, such that the k_1 parameter wants to converge to zero and a_0 wants to converge to negative infinity. To deal with this, we set a lower bound for a_0 of -15, for which the corresponding k_1 estimate was 0.02. In comparison to YFT, the growth rate in both stages is slower for BET, and the transition between stages occurs over a much larger age range (as indicated by the small value of β) but with the midpoint of the transition being at a very similar age to YFT (2.1 yrs, calculated as $a - a_0$). Diagnostic plots for this model are given in Figure B4. As for YFT, the histogram of estimated individual release ages is bi-modal (like the release length distribution) even though a uni-modal log-normal distribution is being assumed (Figure B4(a)). The very slow initial growth is apparent in Figure B4(b), which shows the release and recapture lengths plotted against estimated age, along with the mean fitted growth curve. Because the initial growth stage is almost flat and a_0 is -15, some of the estimated release ages, after being adjusted for a_0, can actually be negative. The release and recapture residuals (Figure B4(c)) suggest the release lengths for very small fish are being underestimated. The residuals for the otolith data (Figure B4(d)) suggest an unbiased but highly variable fit over the limited age range represented in the data.

The transition between growth stages for BET is estimated to be slow (i.e., small β value). In contrast, this parameter was estimated to be high (i.e., quick transition) for YFT and BET, as well as for southern bluefin tuna (Polacheck et al. 2004). Based on this information, and also the fact that Laslett et al. (2002) showed that β can be difficult to estimate accurately, we refit the model for

BET with β fixed at 20. The resulting parameter estimates are given in Table B1. In this case, k_1 is estimated to be 0.15, so still suggesting slow initial growth but not tending to zero. Correspondingly, a_0 no longer tends to negative infinity. The central age of transition ($a - a_0$) is still estimated to occur at about the same age (2.1 years). Diagnostics for this model are shown in Figure B5. There is no longer a problem with negative age estimates (Figure B5(b)). The underestimation in release lengths for small fish is improved, but there is perhaps now a small overestimation in the recapture lengths for these fish (Figure B5(c)). Again, the otolith residuals look fine, but are highly variable (Figure B5(d)).

Because the otolith data for BET do not contain any information about the youngest and oldest fish, giving these data more weight in the likelihood did not lead to sensible results. In particular, the mean asymptotic length parameter wanted to converge to the lower bound that was set for it of 138cm.

Sex information exists for a small number of BET recaptures (38 males, 29 females). As for YFT, these were all recaptures of large fish (ranging from 105 to 158cm) recaptured after a long time at liberty (average of ~4.5 yrs). We did not try fitting sex-specific growth curves for BET (which would again require fixing many parameters); instead, we just highlight the points corresponding to males and females in the fit for the previous model with β fixed (see Figure B6). As with YFT, males appear to grow to a larger size than females, but the difference is not as great.

The mean asymptotic length values ($\mu_{L\infty}$) estimated for BET using all the data seem reasonable (145cm and 151cm in the two models presented in Table B1), especially when the large variability in L_∞ is taken into account (e.g., in the model with β fixed at 20, the estimate of $\sigma_{L\infty}$ is almost 12cm, meaning ~95% of individuals have an L_∞ value in the range of $\mu_{L\infty} \pm 2\sigma_{L\infty}$ = 127 to 175cm). Also, the $\mu_{L\infty}$ values estimated using all data are consistent with the asymptotic lengths suggested by the data for males and females (which was not the case for YFT), lending further support to these values being reasonable for the population as a whole.

Skipjack

Figures S1-S3 for SKJ have somewhat different features than the analogous plots for YFT and BET. Firstly, there is only one clear mode in the release lengths at ~50cm; the times at liberty are less on average (mean 278 days, maximum 1236 days); and the recapture lengths are not much larger than the release lengths, indicating considerably slower growth rates than for YFT or BET (Figure S1). This is confirmed in Figure S2, which shows much smaller changes in length over the same times at liberty. The percent of fish with negative growth increments (at 3%) is highest for SKJ. Although the plot of growth rate versus release length (Figure S3) has a different pattern than the analogous plot for YFT and BET, it still shows a clear change-point in growth around 45cm, suggesting a two-stanza model is more appropriate for SKJ as well.

Based on these findings, we fit a VB log k model to the SKJ tag-recapture data; the parameter values obtained are given in Table S1. Once again, the results were sensitive to starting values, probably because the surface of the likelihood near the maximum appears to be quite flat. In contrast to YFT and BET, the estimates of k_1 and k_2 for SKJ indicate very quick growth in the first stage followed by much slower growth in the second stage. Diagnostic plots are given in Figure S4. Note that without

otolith data a_0 could not be estimated directly from the model; therefore, we calculated it after fitting the model (using parameter estimates obtained from the model) such that the length of a fish at age 0 is 20cm. A value of 20cm at age 0 has been suggested for previous analyses (e.g., Eveson 2011) as being reasonable, but it is fairly arbitrary and can influence interpretation of the diagnostic plots, so this needs to be kept in mind when looking at Figure S4. For SKJ, the estimated release ages have a uni-modal distribution (FigureS4(a)), as suggested by the distribution of release lengths. Figure S4(b) shows the release and recapture lengths plotted against estimated age, along with the mean fitted growth curve, from which the rapid initial growth up to about age 1 followed by much slower growth is apparent . The release and recapture residuals show a reasonably good fit, although there appears to be a small underestimate in length at age prior to the transition point (Figure S4(c)).

Discussion

The results presented here suggest that a two-stanza growth model allowing for a change in the underlying growth function at a given age is appropriate for YFT, BET and SKJ in the Indian Ocean. The 'VB log k' growth function developed in Laslett et al. (2002) appears to be a reasonable choice. It has been suggested that differential size-selectivity between the FAD and free-set components of the purse-seine fishery could result in the apparent two-stanza growth (Kolody 2008). If this is true, our investigation suggests it is not the primary contributor for YFT because the two-stage pattern in growth is evident when looking at the tag-recapture data from either component of the fishery separately.

Several variations of the VB log k growth model were fit to the YFT tag-recapture and otolith data. Which model is best needs further discussion, but in all cases the results suggest slower growth up to about age 2, followed by very rapid growth. In comparison, the results for BET suggest slower growth than YFT during both stages, but still quicker in the second stage and with the transition occurring around age 2. Males appear to grow to a larger size than females for both BET and YFT, but this difference is greater for YFT. The results for SKJ suggest that, unlike YFT or BET, they grow very rapidly up to about age 1, then much more slowly afterwards.

In fitting the VB log k growth models to all species, we encountered convergence problems and sensitivity to starting values. This can partly be attributed to the large variability in the tag-recapture data. Much of this variability is likely to be real, since fish experiencing different conditions may well experience very different growth trajectories; however, there are also many fish recorded as having unrealistically fast or slow growth, and some with negative growth (even for long times at liberty). These points are difficult for the model to fit. For example, the LEP method deals with fish that have negative or very slow growth over long times at liberty by estimating their age at release to be high and their asymptotic length to be low, because it is only when fish get old and approach their asymptotic length that they experience such a small amount growth. These points are indicated for YFT in Figures Y4(b) andY5(b), for BET in Figures B4(b) and B5(b), and for SKJ in Figure S4(b).

In general, we found the tag-recapture data and otolith data for YFT to be consistent, except at very small lengths (<45cm), in which case the otolith data suggest YFT are smaller initially but grow more rapidly. For BET, the length range of fish for which we have otolith data is limited, with no very small or very large fish, so it is difficult to assess its consistency with the tag-recapture data. Furthermore,

it is important to recognize that the otolith age estimates used in the models may be biased due to potential reader effects that were not taken into account (see footnote 3). It should also be noted that the otolith readings used here are not consistent with the readings for Western Indian Ocean YFT and BET presented in Stéquert et al. (1996) and Stéquert and Conand (2004), which suggest larger lengths at age for both species. This has been noted previously (Morize et al. 2008), but the reason is still not clear.

Acknowledgments

A large number of people were involved in the collection and production of data used in this report. For the otolith data, Eric Morize, Jean-Marie Munaron, Maylis Labonne, and Carys Davies all contributed to the readings; Patrice Dewals and his team and Juanjo Areso were involved in otolith collection; and Emmanuel Chassot was a coordinator and collaborator in the project. Numerous scientific staff and members of the fishing industry were involved in the release and recapture stages of the Indian Ocean Tuna Tagging Programme, and we are grateful for all their efforts.

References

Dortel, E., Sardenne, F., Le Croizier, G., Million, J., Rivot, E., Bousquet, N., and Chassot, E. 2012. Integrated growth for yellowfin and bigeye tunas of the Indian Ocean: Conflicting information from different data sources. IOTC-2012-WPTT14-24.

Eveson, J.P., Polacheck, T., and Laslett, G.M. 2007. Consequences of assuming an incorrect error structure in von Bertalanffy growth models: a simulation study. Can. J. Fish. Aquat. Sci. 64: 602-617.

Eveson, J.P. and Million, J. 2008a. Estimation of growth parameters for yellowfin, bigeye and skipjack tuna using tag-recapture data. IOTC-2008-WPTDA-07.

Eveson, J.P. and Million, J. 2008b. Results from applying the Laslett, Eveson and Polacheck (LEP) method to the data agreed on at the IOTC Working Party of Tagging Data Analysis. IOTC-2008-WPTDA-07-add1.

Eveson, J.P. 2011. Updated growth estimates for skipjack obtained from the LEP method applied to the most recent RTTP-IO tag-recapture data. *Appendix to*: Preliminary application of the Brownie-Petersen method to skipjack tag-recapture data. IOTC-2011-WPTT13-30Rev_1.

Fabens, A.J. 1965. Properties and fitting of the von Bertalanffy growth curve. Growth 29: 265-289.

Fonteneau, A. and Gascuel, D. 2008. Growth rates and apparent growth curves for yellowfin, skipjack and bigeye tagged and recovered in the Indian Ocean during the IOTTP. IOTC-2008-WPTDA-08.

Francis, R.I.C.C. 1988. Maximum likelihood estimation of growth and growth variability from tagging data. N.Z. J. of Mar. Freshwater Res. 22: 42-51.

Hallier, J.P. 2008. Status of the Indian Ocean Tuna Tagging Programme – RTTP-IO. IOTC-2008-WPTDA-10.

Hearn, W.S. and Polacheck, T. 2003. Estimating long-term growth-rate changes of southern bluefin tuna (*Thunnus maccoyii*) from two periods of tag-return data. Fish. Bull. 101: 58-74.

Hillary, R.M., Million, J., and Anganuzzi, A. 2008. Exploratory modelling of Indian Ocean tuna growth incorporating both mark-recapture and otolith data. IOTC-2008-WPTDA-03.

IOTC-WPTT13. 2011. Report of the Thirteenth Session of the IOTC Working Party on Tropical Tunas. Lankanfinolhu, North Malé Atoll, Republic of Maldives, 16–23 October 2011. IOTC-2011-WPTT13-R[E]: 94 pp.

James, I.R. 1991. Estimation of von Bertalanffy growth curve parameters from recapture data. Biometrics 47: 1519-1530.

Kolody, D. 2011. Can length-based selectivity explain the two stage growth curve observed in Indian Ocean YFT and BET? IOTC-2011-WPTT13-33.

Laslett, G.M., Eveson, J.P., and Polacheck, T. 2002. A flexible maximum likelihood approach for fitting growth curves to tag-recapture data. Can. J. Fish. Aquat. Sci. 59: 976-986.

Laslett G.M., Eveson, J.P., and Polacheck, T. 2004. Estimating the age at capture in capture-recapture studies of fish growth. Aust. N.Z. J. Stat. 46: 59-66.

Leroy, B. 2000. Preliminary results on skipjack (*Katsuwonus pelamis*) growth. 13th Meeting of the Standing Committee on Tuna and Billfish (SCTB13), Noumea, New Caledonia, 5-12 July 2000. Working paper SKJ-1.

Morize, E., Munaron, J.M., Hallier, J.P., and Million J. 2008. Preliminary growth studies of yellowfin and bigeye tuna (*Thunnus albacares* and *T. obesus*) in the Indian Ocean by otolith analysis. IOTC-2008-WPTT-30.

Palmer, M.J., Phillips, B.F., and Smith, G.T. 1991. Application of nonlinear models with random coefficients to growth data. Biometrics 47: 623-635.

Polacheck, T., Eveson, J.P., and Laslett, G.M. 2004. Increase in growth rates of southern bluefin tuna (*Thunnus maccoyii*) over four decades: 1960 to 2000. Can. J. Fish. Aquat. Sci. 61: 307-322.

Sainsbury, K.J. 1980. Effect of individual variability on the von Bertalanffy growth equation. Can. J. Fish. Aquat. Sci. 37: 241-247.

Stéquert, B., Panfili, J., and Dean, J.M. 1996. Age and growth of yellowfin tuna, *Thunnus albacares*, from the Western Indian Ocean, based on otolith microstructure. Fish. Bull. U.S., 94: 124-134.

Stéquert, B. and Conand, F. 2004. Age and growth of bigeye tuna (*Thunnus obesus*) from the Western Indian Ocean. Cybium, 28: 163-170.

Wang, Y.-G., Thomas, M.R., and Somers, I.F. 1995. A maximum likelihood approach for estimating growth from tag-recapture data. Can. J. Fish. Aquat. Sci. 52: 252-259.

Figures and Tables

Table Y1. Parameter estimates from fitting a VB log k growth model jointly to the tag-recapture and otolith data for YFT. W=factor by which the otolith likelihood was multiplied.

Model	W	mu.Linf	sig.Linf	k1	k2	alpha	beta	mu.A	sig.A	sig.tag	a0	sig.oto
1	1	132.3	10.1	0.20	1.51	3.5	15.6	1.06	0.14	3.9	-1.3	11.9
2	100	129.8	19.3	0.31	1.58	2.5	20^	0.65	0.17	3.9	-0.3	1.0*
3	1	145#	10.4	0.15	0.94	3.8	20^	1.18	0.13	4.3	-1.7	12.8
4	100	145#	21.7	0.26	0.85	2.4	20^	0.67	0.16	4.6	-0.3	1.0*

*Estimate on lower bound
^Estimate on upper bound
Fixed

Table Y2. Parameter estimates from fitting a VB log k growth model to the tag-recapture and otolith data for YFT for males and females separately. The data with sex information (53 males; 32 females) are insufficient for estimating all parameters freely, so several parameters (as indicated by shading) were fixed at the maximum likelihood estimates from the joint tag and otolith fit to all data with the otolith data highly weighted (i.e., Table 1, row 2).

Sex	mu.Linf	sig.Linf	k1	k2	alpha	beta	mu.A	sig.A	sig.tag	a0	sig.oto
M	150.0	8.59	0.26	0.95	2.5	20^	0.65	0.17	1.0*	-0.3	n/a
F	140.3	8.64	0.28	0.92	2.5	20^	0.65	0.17	1.7	-0.3	n/a

* Estimate on lower bound
^ Estimate on upper bound

Table B1. Parameter estimates from fitting a VB log k growth model jointly to the tag-recapture and otolith data for BET.

Model	mu.Linf	sig.Linf	k1	k2	alpha	beta	mu.A	sig.A	sig.tag	a0	sig.oto
1	145.5	9.5	0.02	0.55	17.1	2.3	2.8	0.03	2.9	-15*	10.5
2	150.9	11.7	0.15	0.41	3.4	20#	1.02	0.14	3.1	-1.2	7.8

*Estimate on lower bound
Fixed

Table S1. Parameter estimates from fitting a VB log k growth model to the tag-recapture data for SKJ.

mu.Linf	sig.Linf	k1	k2	alpha	beta	mu.A	sig.A	sig.tag	a0*
71.6	4.9	1.12	0.33	0.95	24.8	0.22	0.23	1.7	-0.3

* Without otolith data, the a0 parameter cannot be estimated directly from the model so it was calculated post model fitting such that length at age 0 is 20cm.

Figure Y1. Histograms of (a) release length; (b) recapture length; (c) days at liberty for YFT.

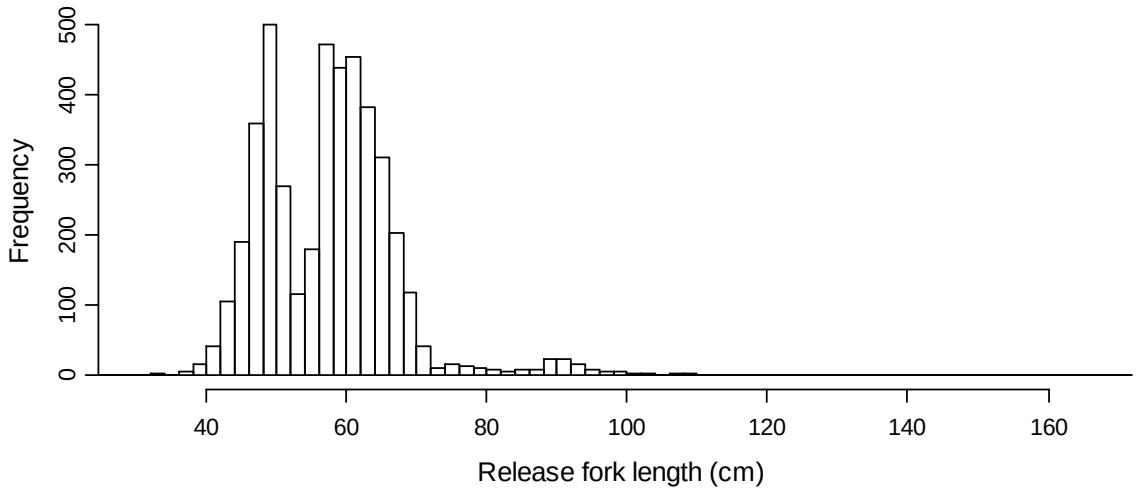

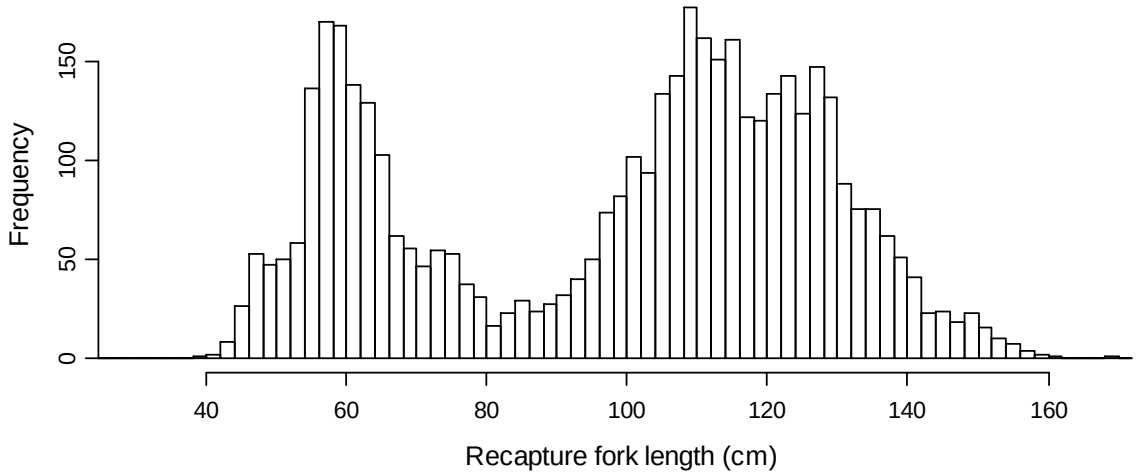

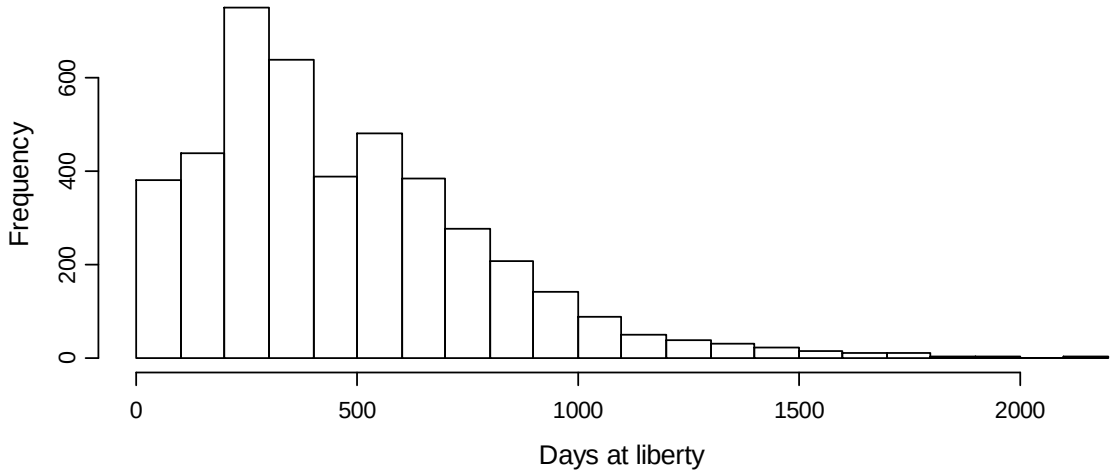

Figure Y2. Length increment (recapture length -release length) vs. days at liberty for YFT.

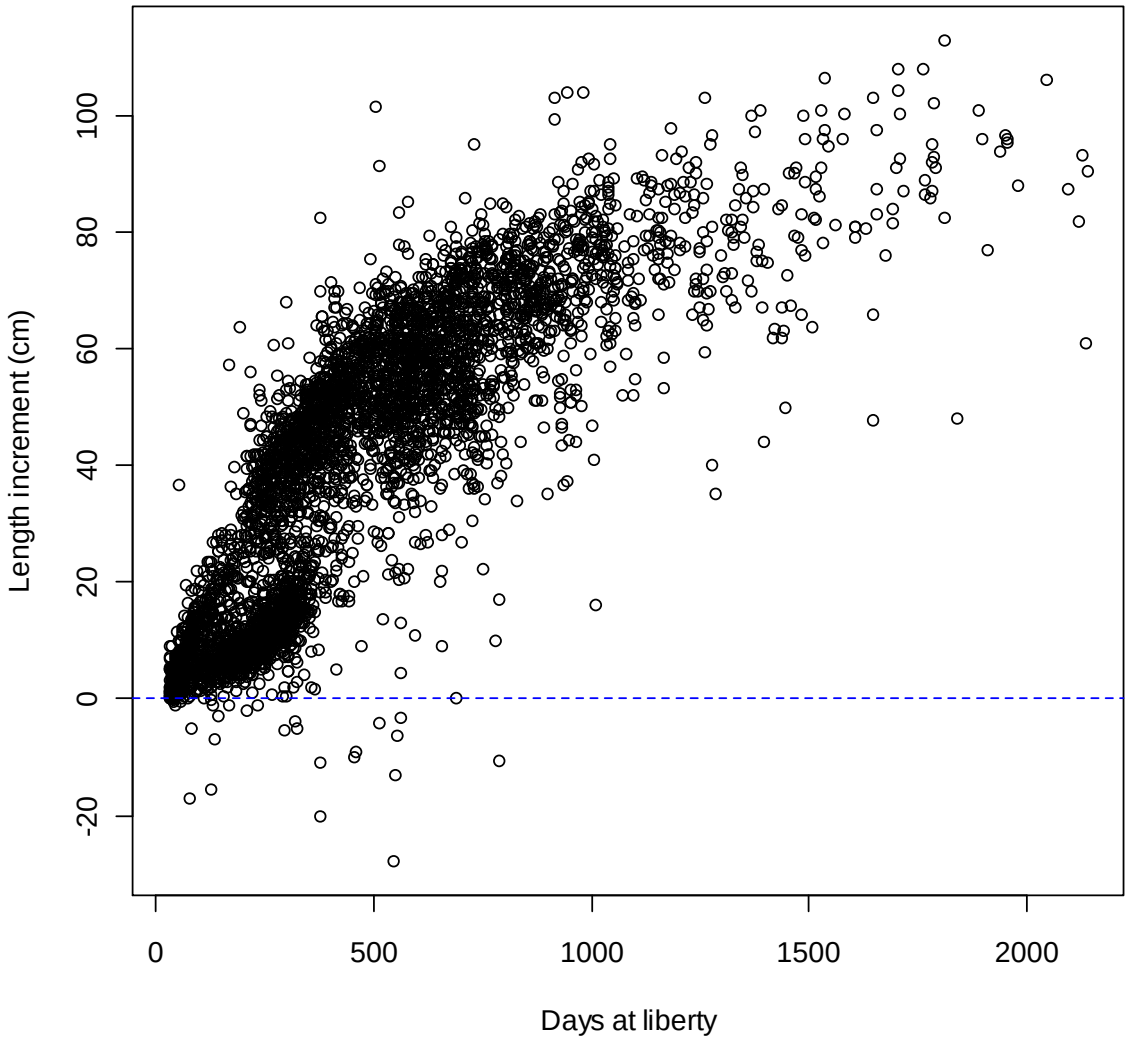

Figure Y3. (a) Growth rate vs. release length for YFT. For VB growth, the growth rate should decline linearly as release length increases, so this plot suggests a 2-stage growth model is more appropriate for YFT. (b) Same as (a) but showing growth rate of recaptures coming from FAD purse-seine catches versus free-school purse-seine catches. The marked change in growth rate with length is clear for both types of catches, suggesting differential size-selectivity is not the cause of the apparent 2-stage growth.

(a)

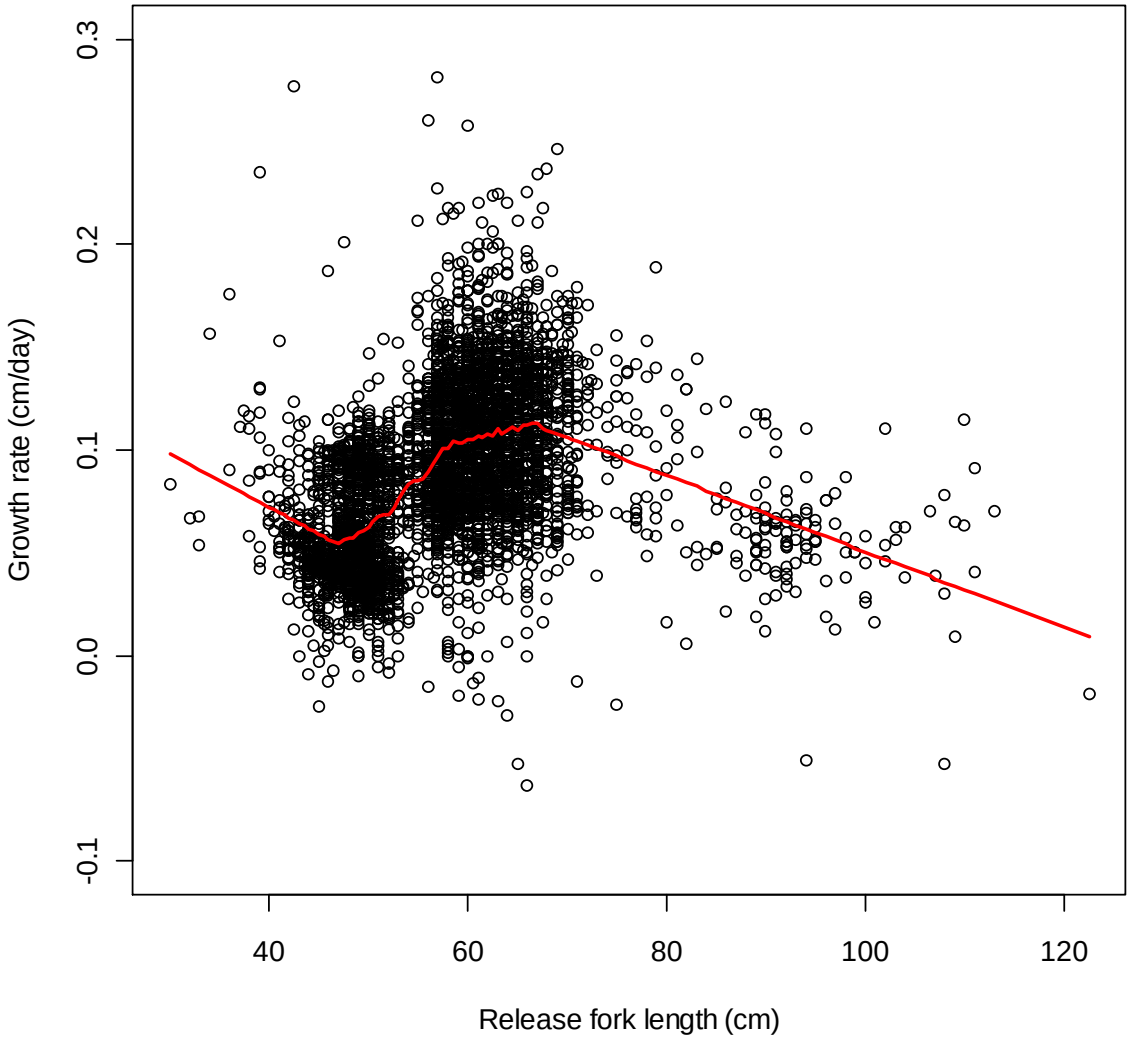

(b)

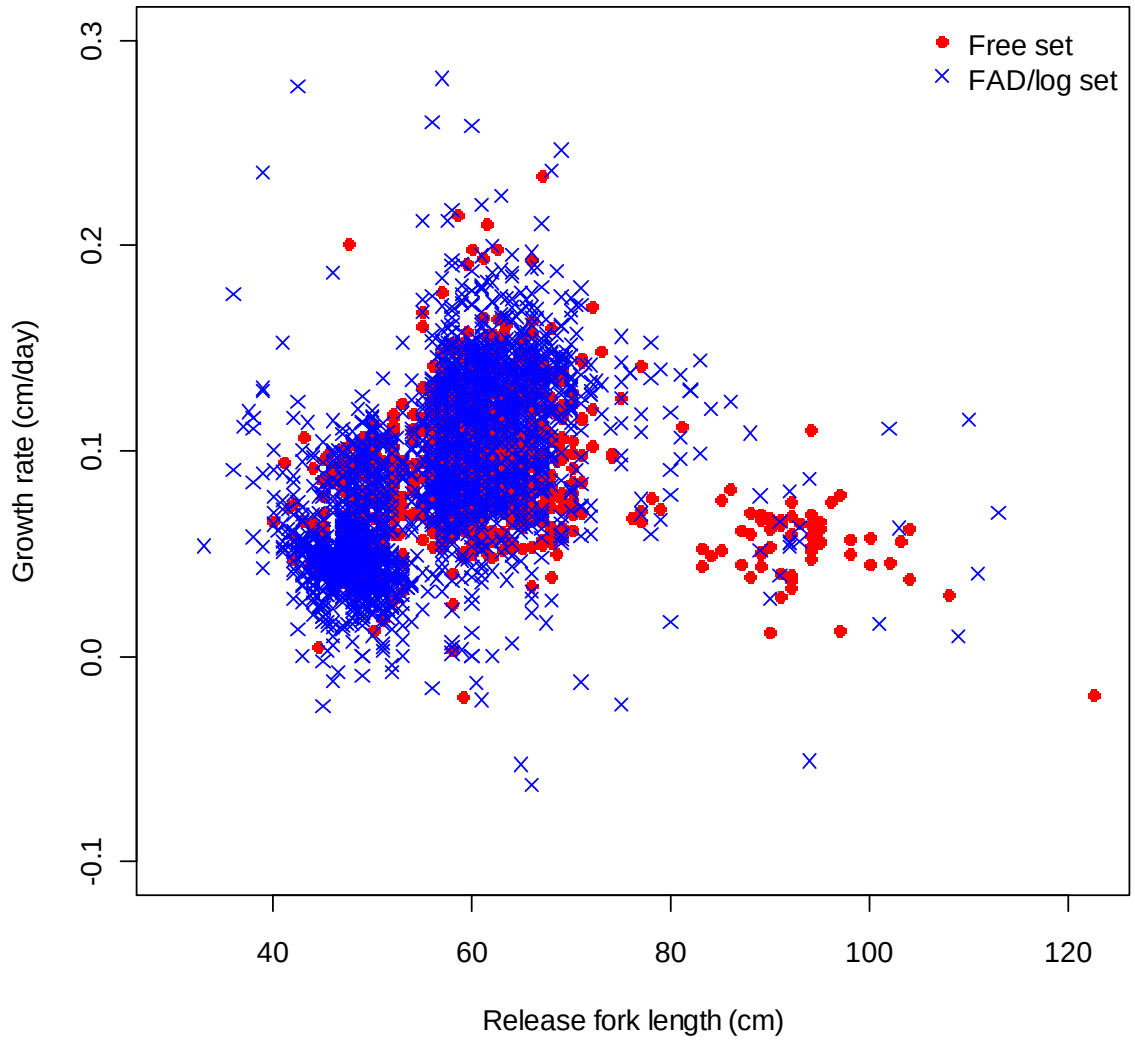
Free set
FAD/log set
Growth rate (cm/day)
0.3
0.2
0.1
0.0
-0.1
40
60
80
100
120
Release fork length (cm)

Figure Y4 (a-d). Results from fitting a VB log k model jointly to the YFT tag-recapture and otolith data assuming a log normal distribution for the release ages.

(a) Estimated release age distribution (green line) overlaying conditionally unbiased estimates of individual release ages.

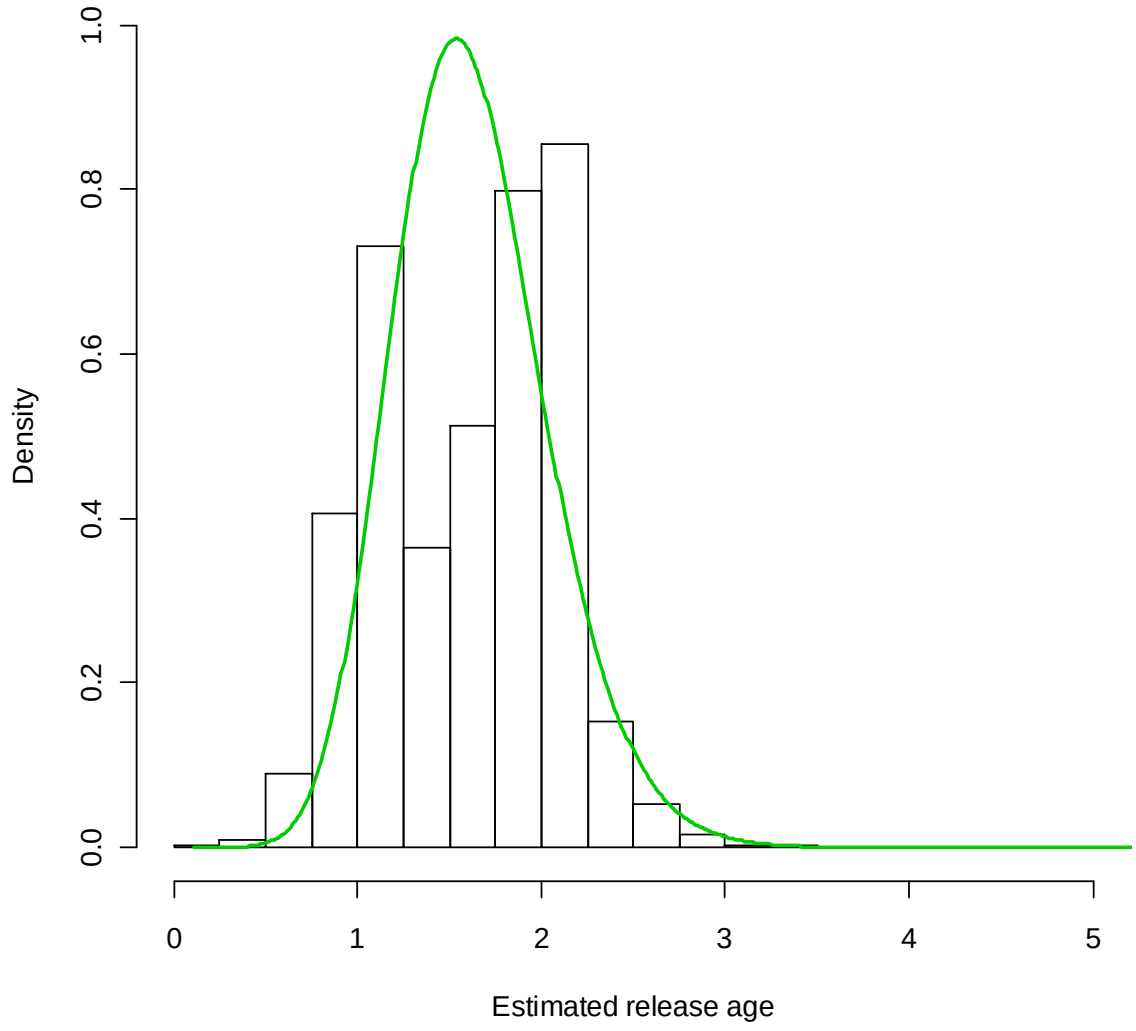

(b) Estimated mean growth curve (black line) and data, Red circles = release points; green triangles=recapture points; blue stars=otolith data. Note that release ages are estimated as in (a), and recapture ages equal estimated release age plus time at liberty. The line segments show fish with negative growth, and explain why some release ages are estimated unrealistically high.

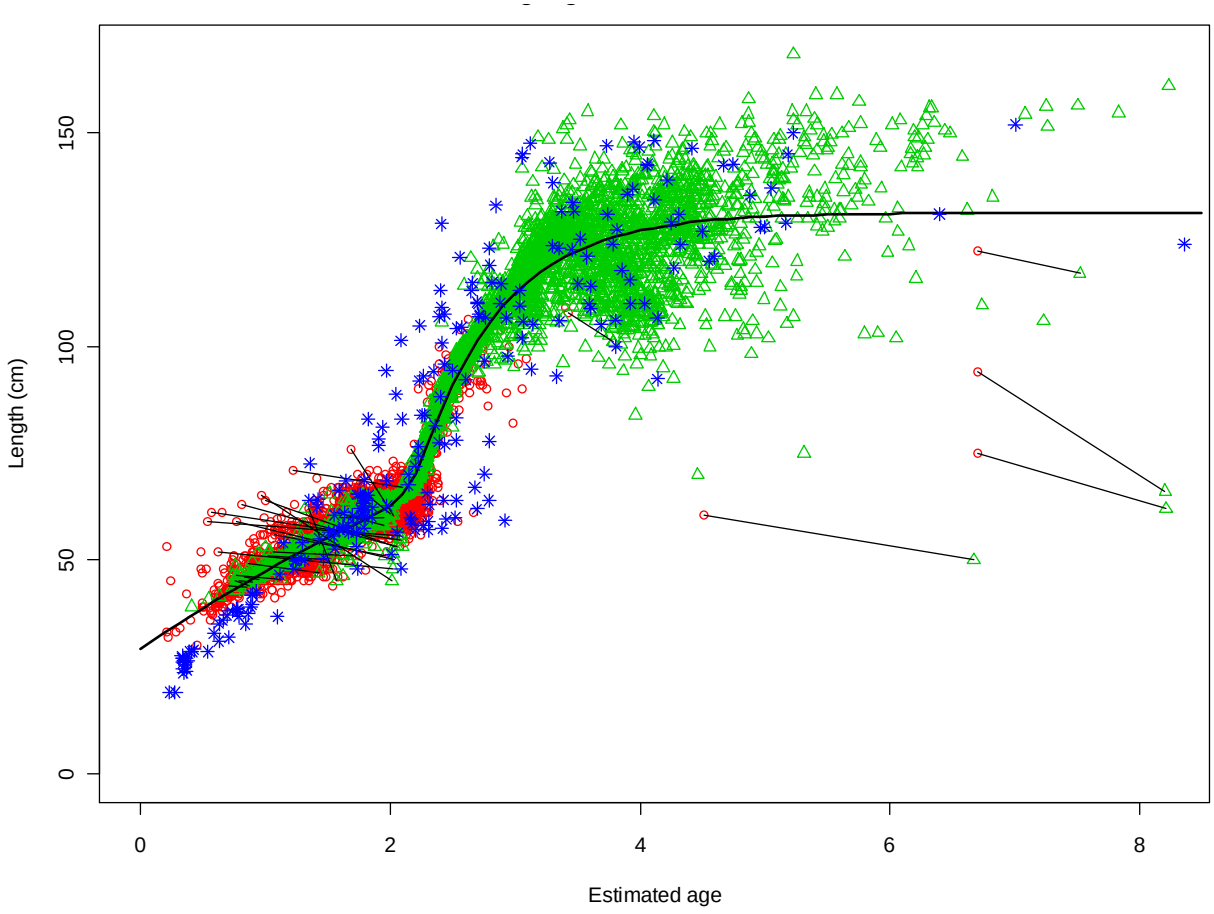

(c) Residuals for tag-recapture data.

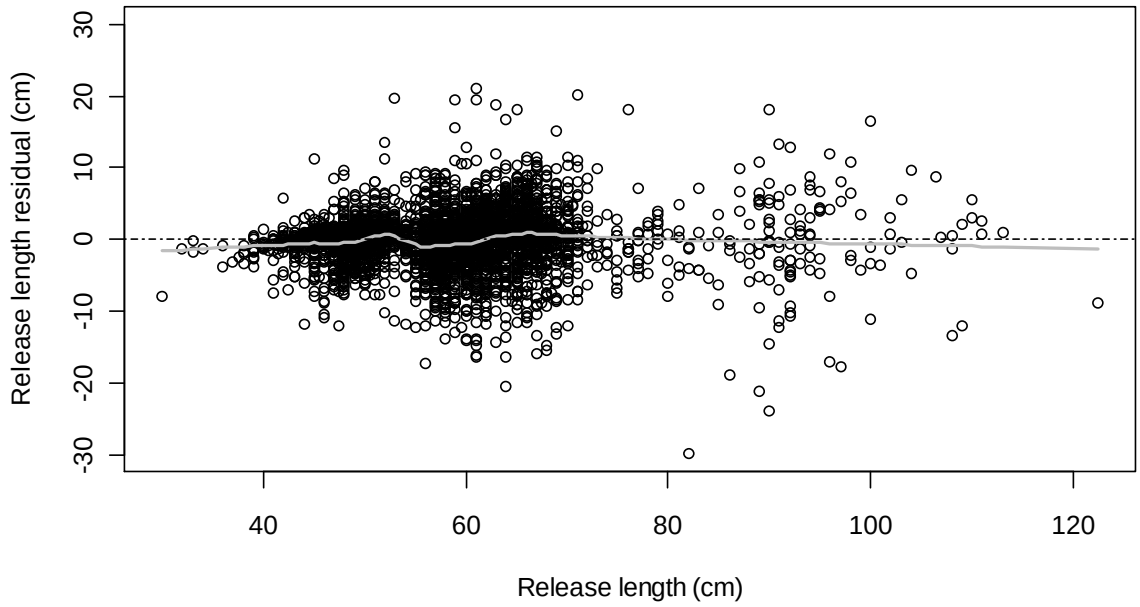

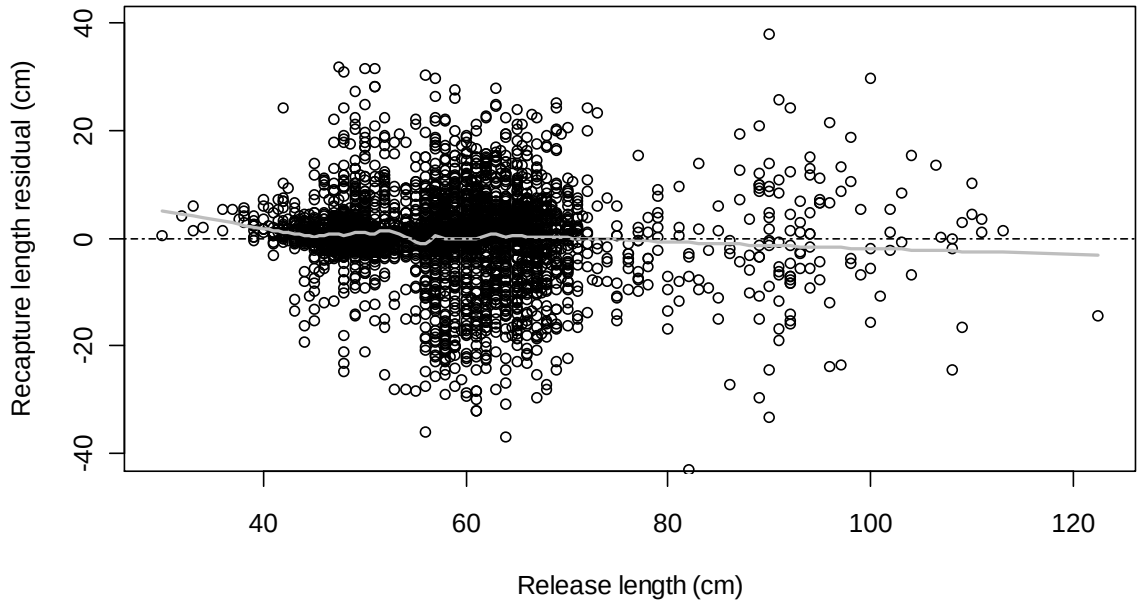

(d) Residuals for otolith data.

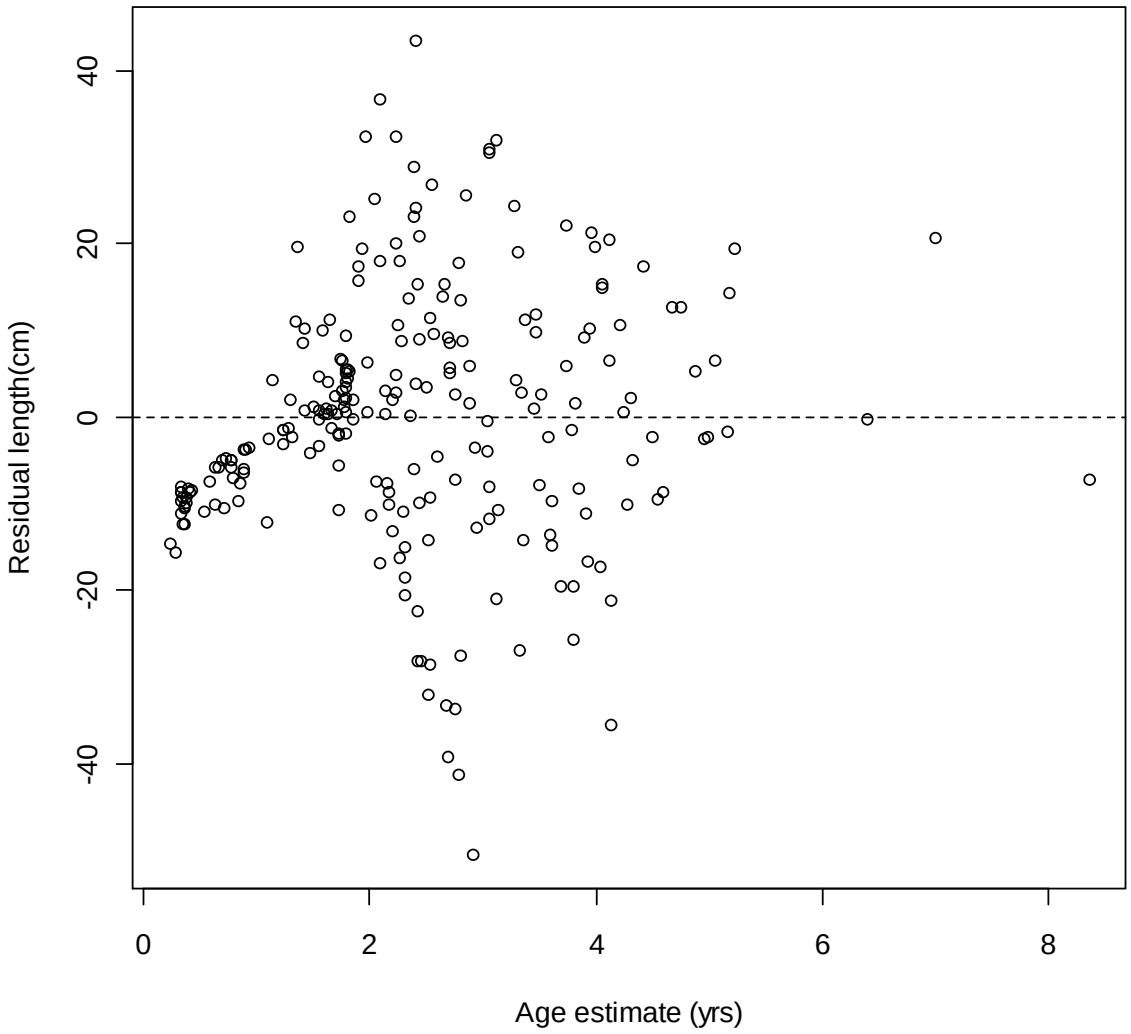

Figure Y5 (a-d). Results from fitting a VB log k model jointly to the YFT tag-recapture and otolith data assuming a log normal distribution for the release ages, and highly weighting the otolith likelihood by a factor of 100 (i.e., W=100) to make it have greater influence than the tag-recapture data since otherwise the tag-recapture data dominates.

(a) Estimated release age distribution (green line) overlaying conditionally unbiased estimates of individual release ages (W=100).

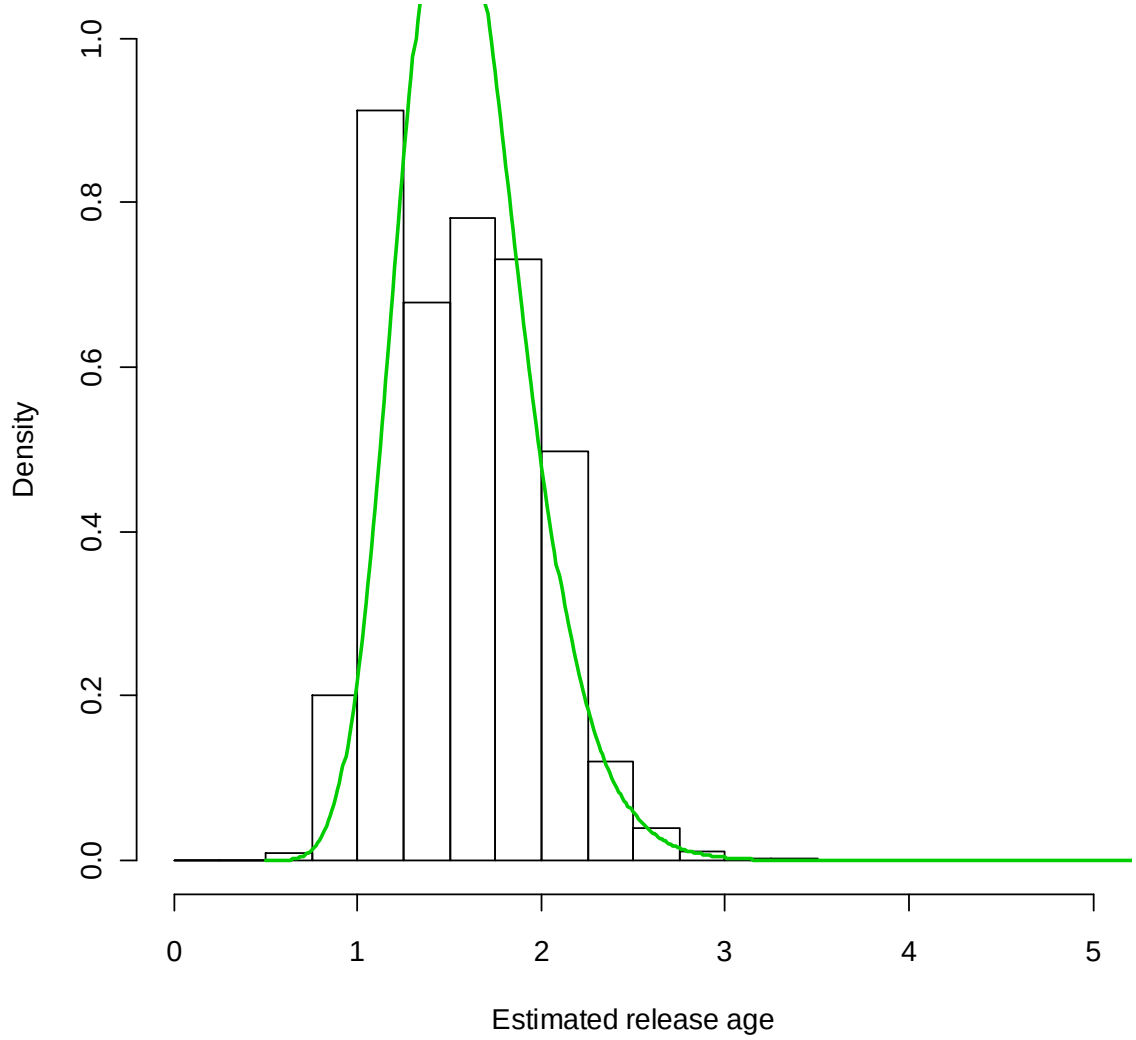

(b) Estimated mean growth curve (black line) and data (W=100). Red circles = release points; green triangles=recapture points; blue stars=otolith data. Note that release ages are estimated as in (a), and recapture ages equal estimated release age plus time at liberty. The line segments show fish with negative growth, and explain why some release ages are estimated unrealistically high.

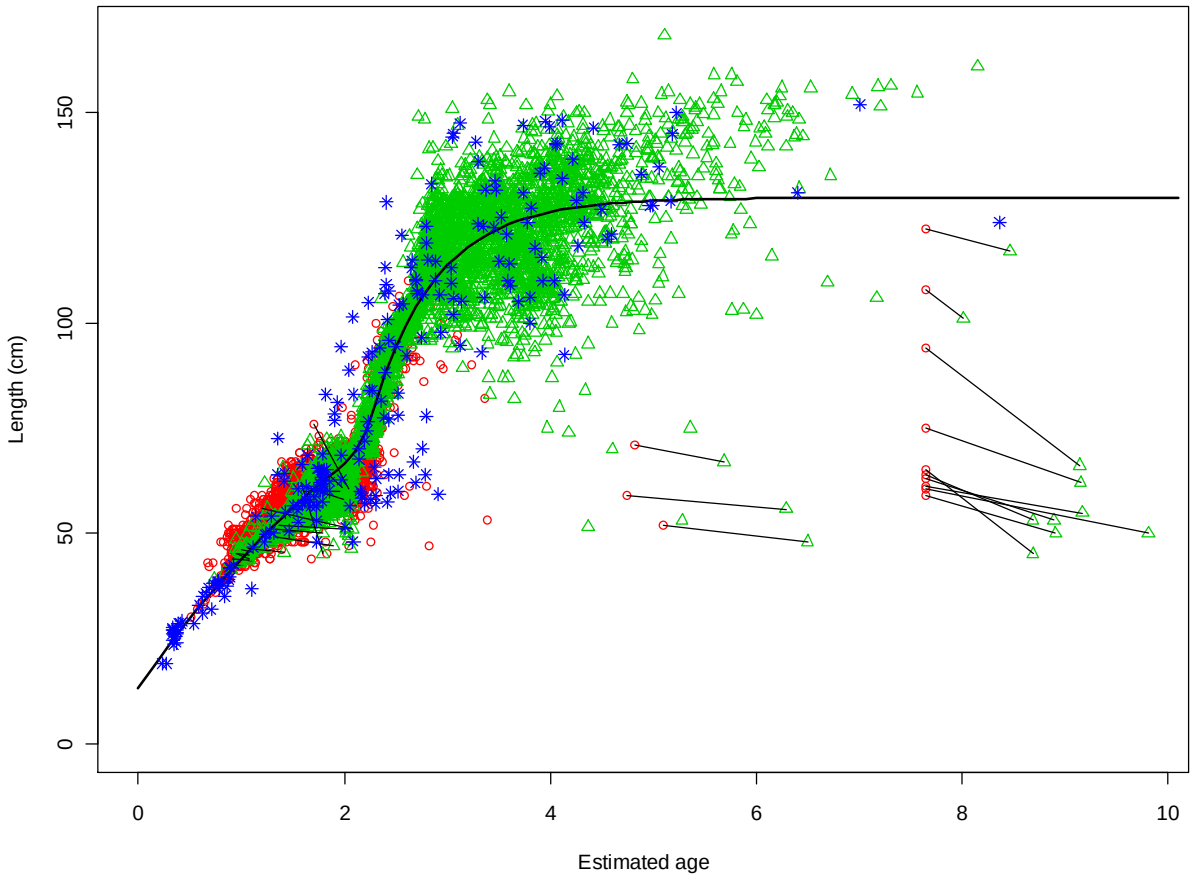

(c) Residuals for tag-recapture data (W=100).

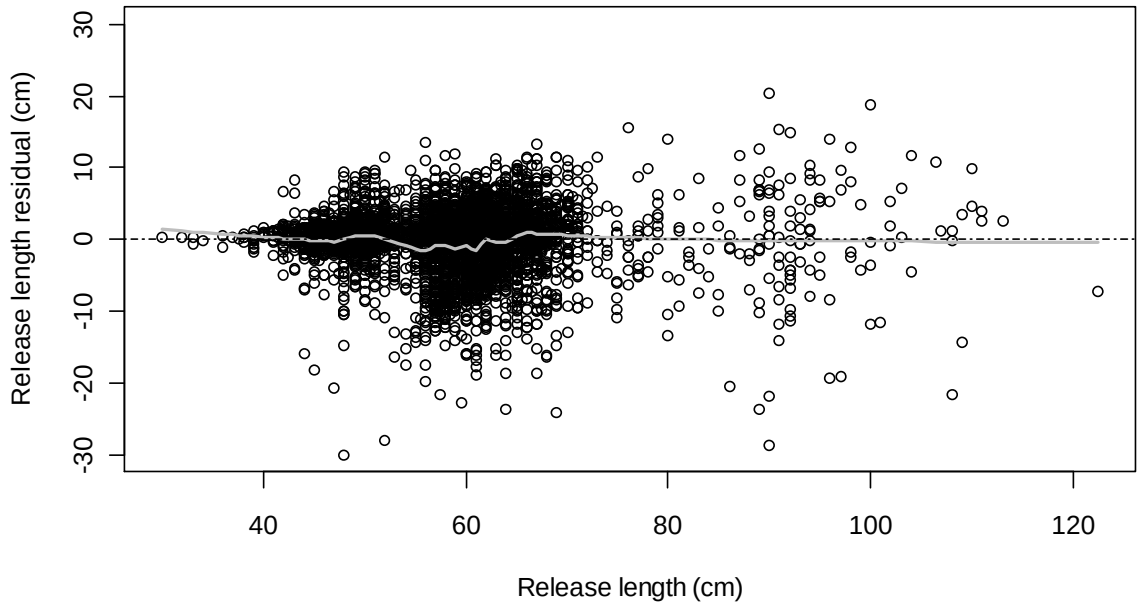

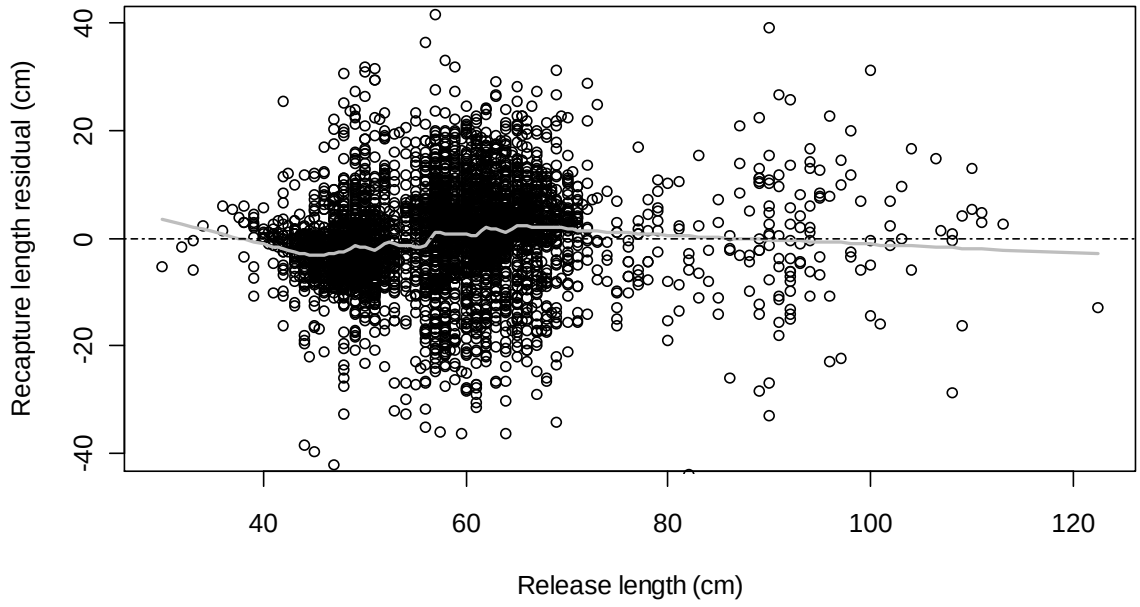

(c) Residuals for otolith data (W=100).

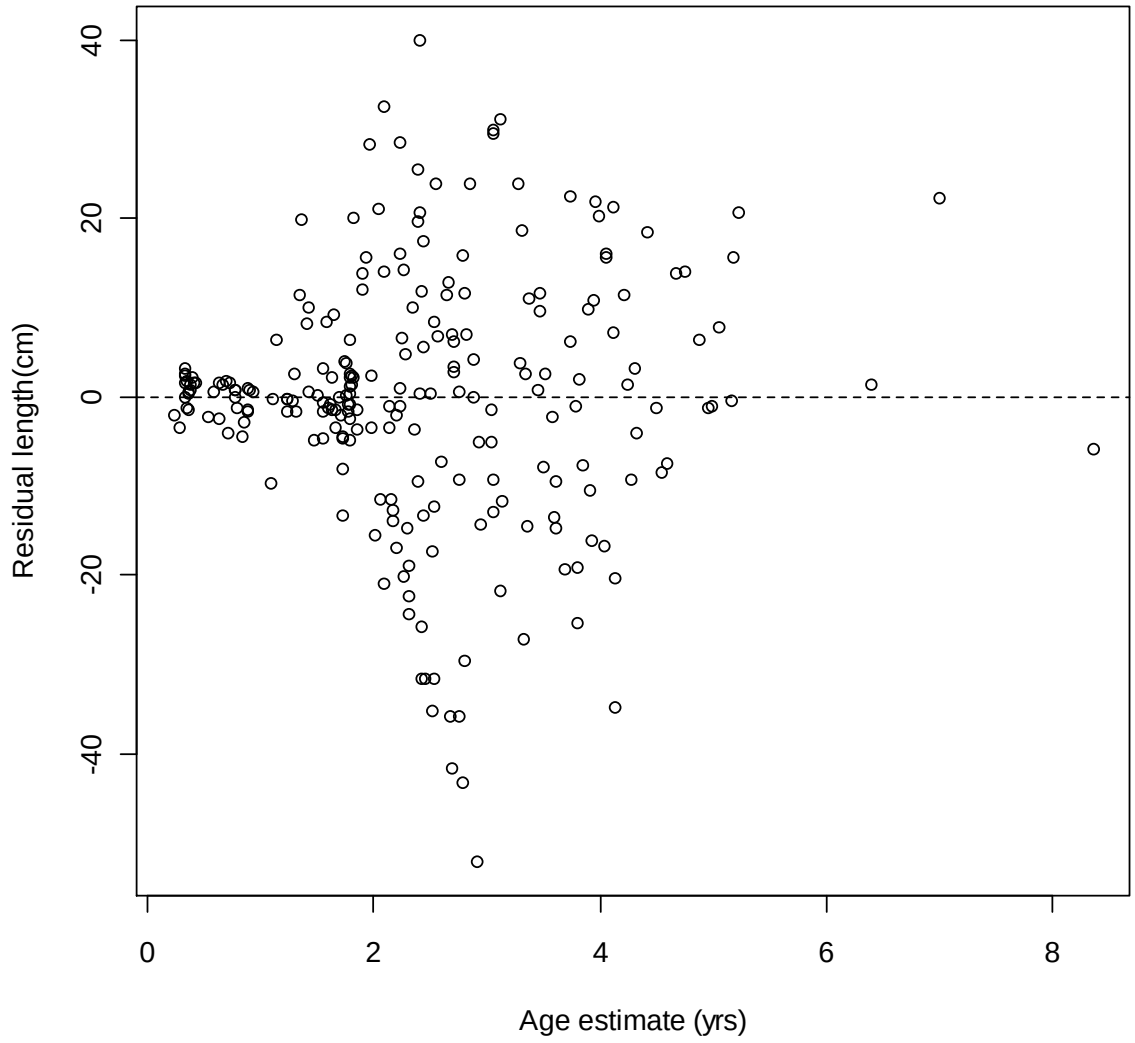

Figure Y6. Estimated mean VB log k growth curve and tag-recapture data for males (light blue; n=53) and females (pink; n=32). The models were fit by fixing some parameters at the estimates from the joint fit to all data (see Table 2).

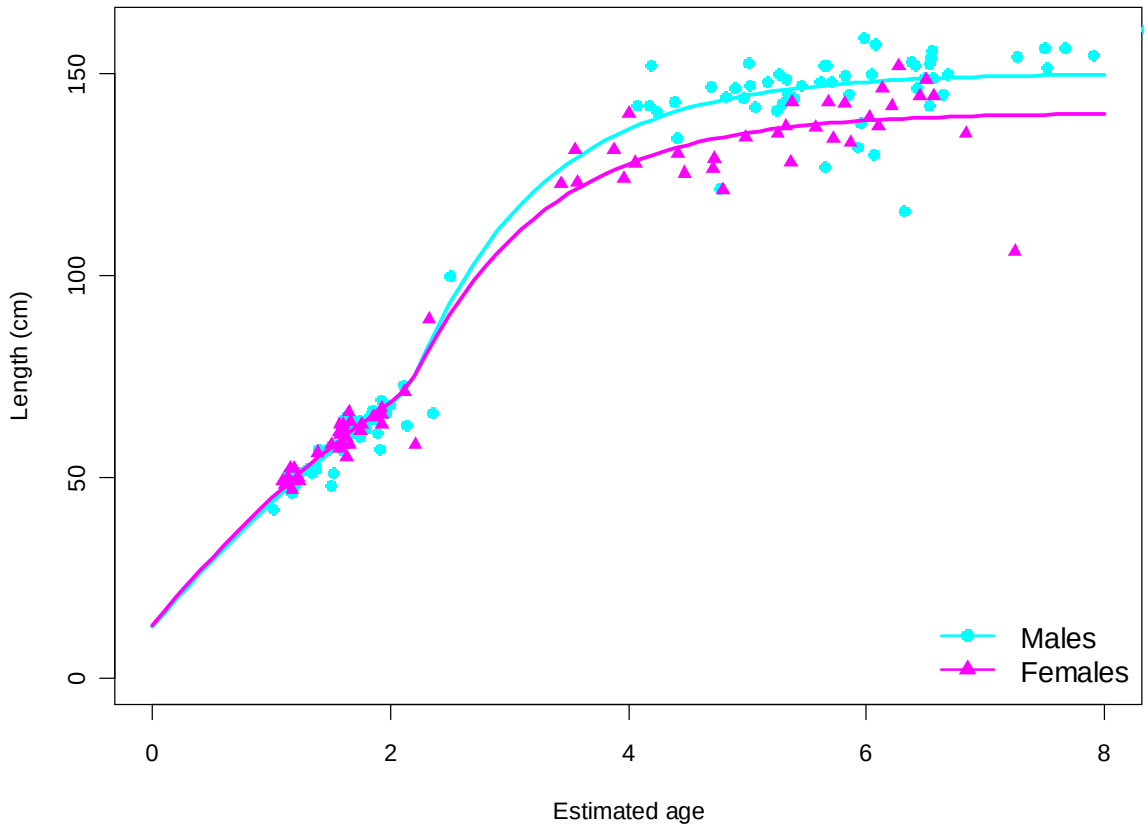

Figure Y7. Comparison of the mean VB log k growth curves estimated for YFT, as given in Table 1 and Table 2.

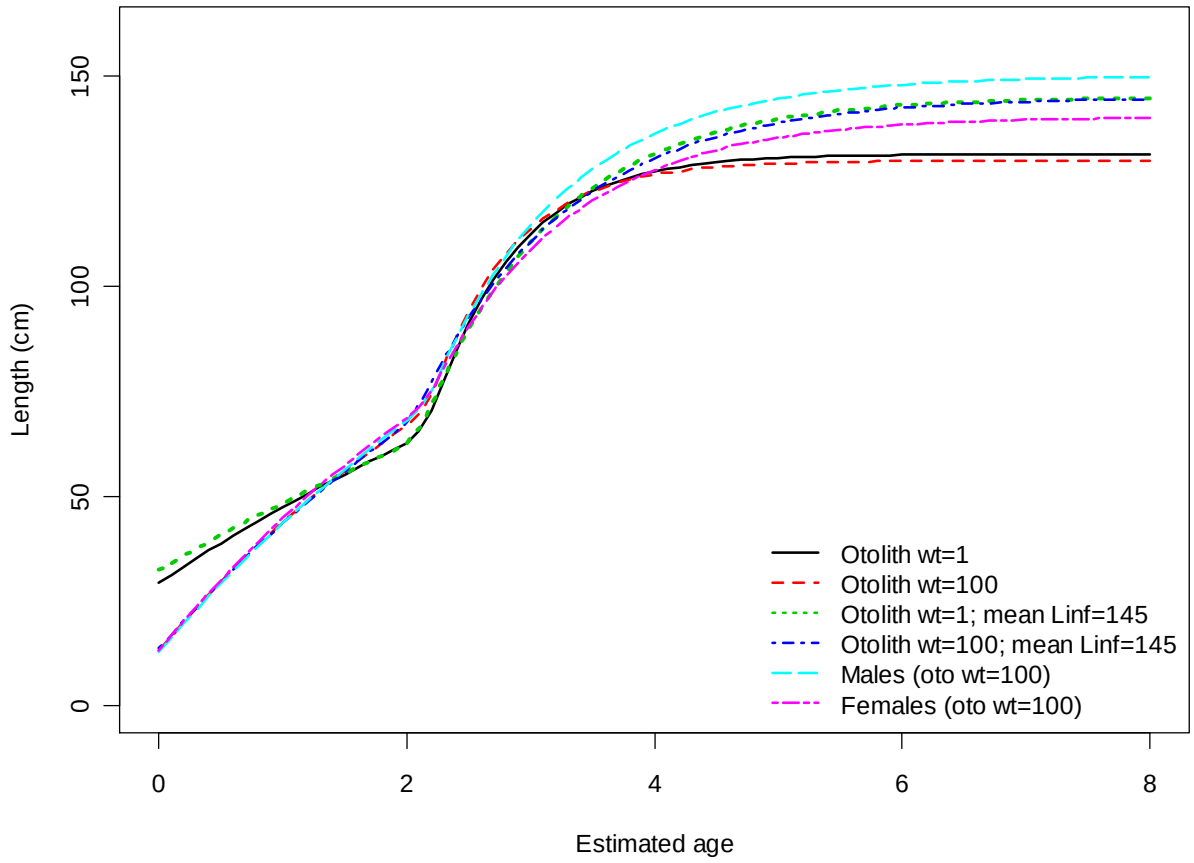

Figure B1. Histograms of (a) release length; (b) recapture length; (c) days at liberty for BET.

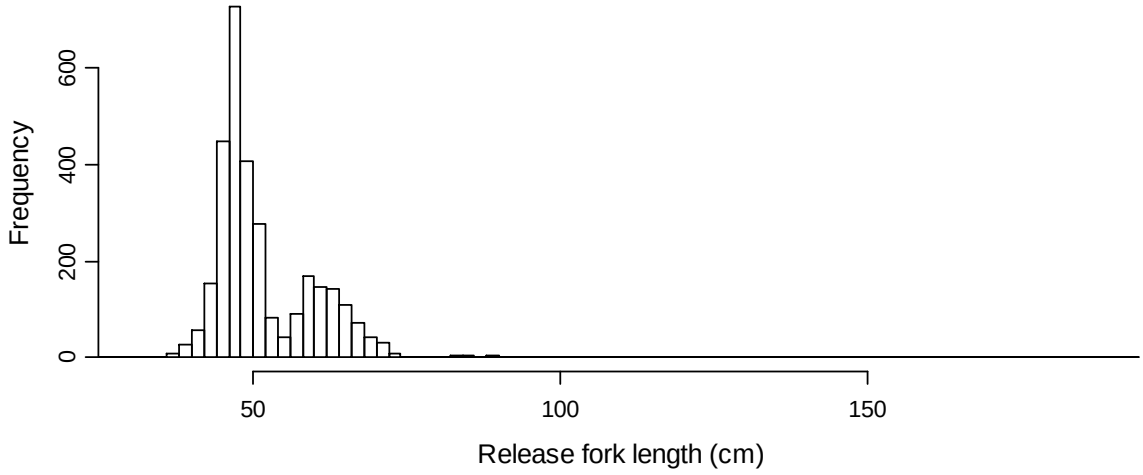

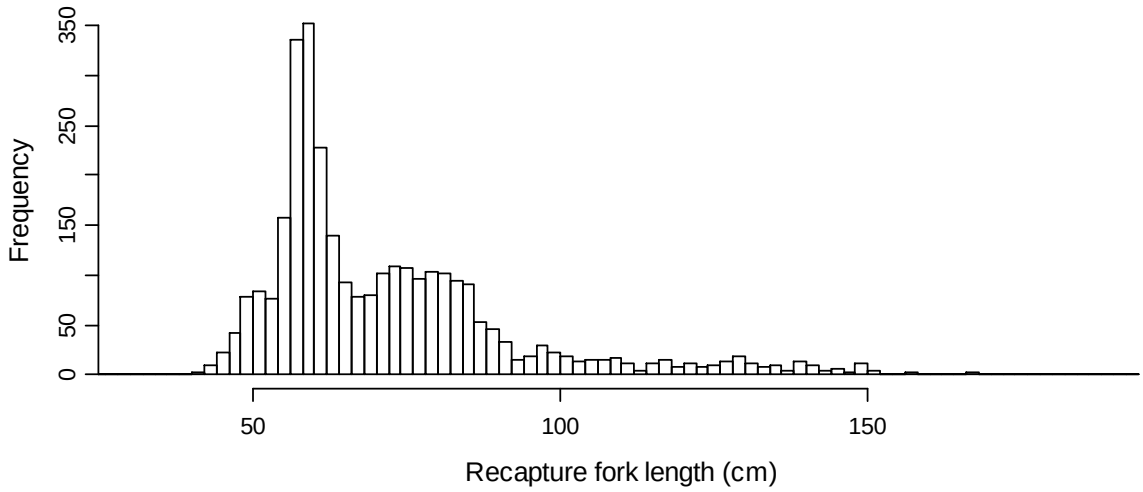

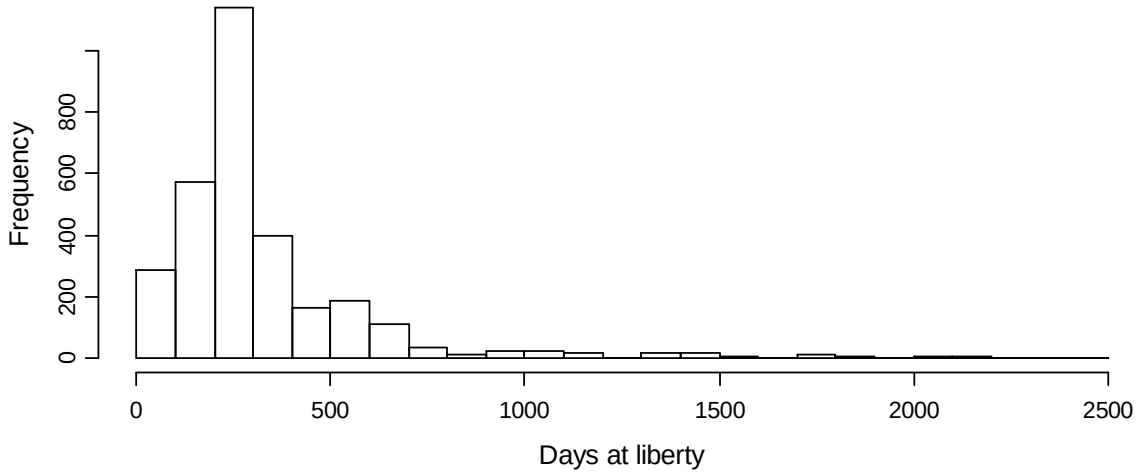

Figure B2. Length increment (recapture length-release length) vs. days at liberty for BET.

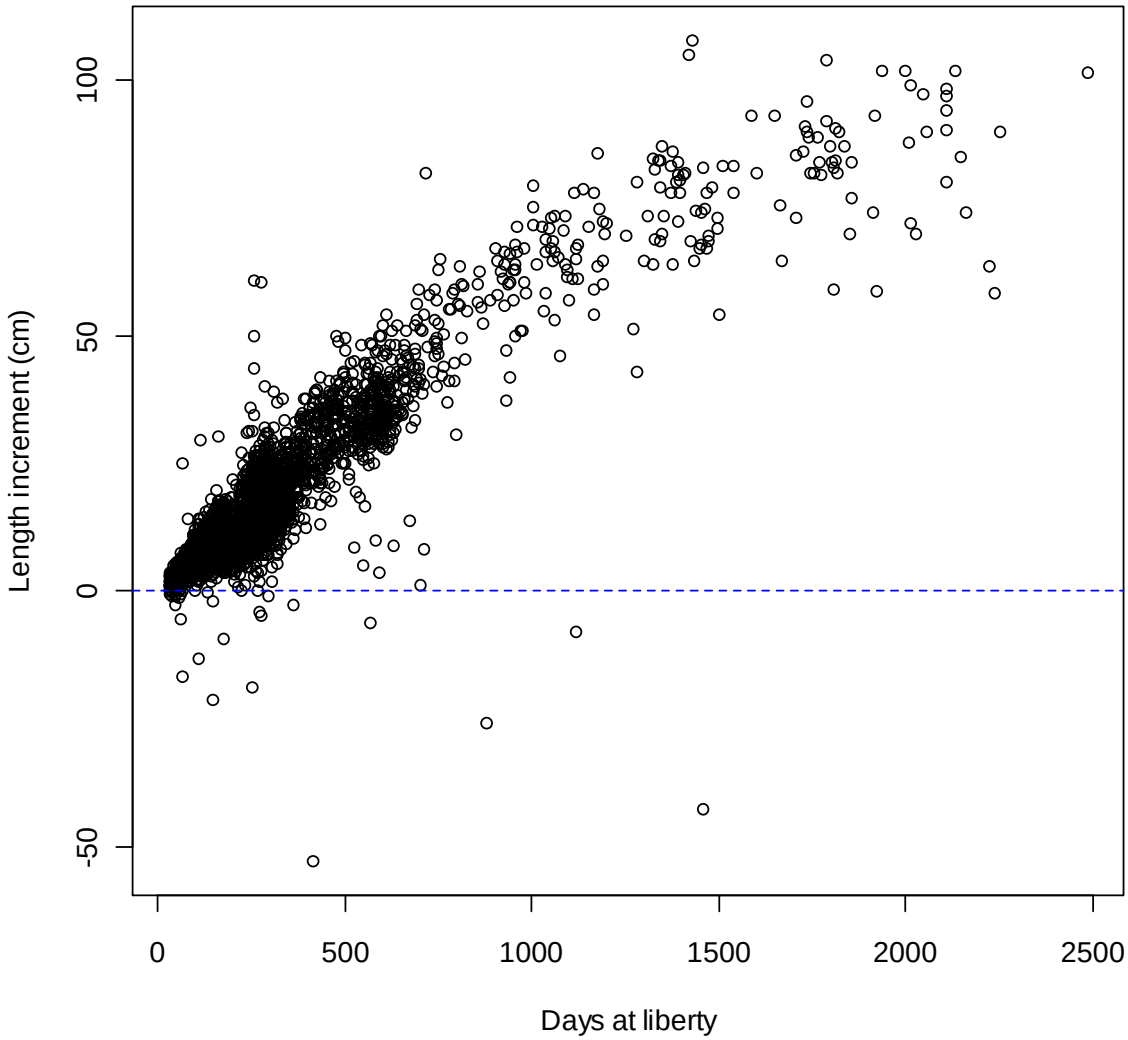

Figure B3. Growth rate vs. release length for BET. As for YFT (Figure Y3), this plot suggests a 2-stage growth model is appropriate for BET.

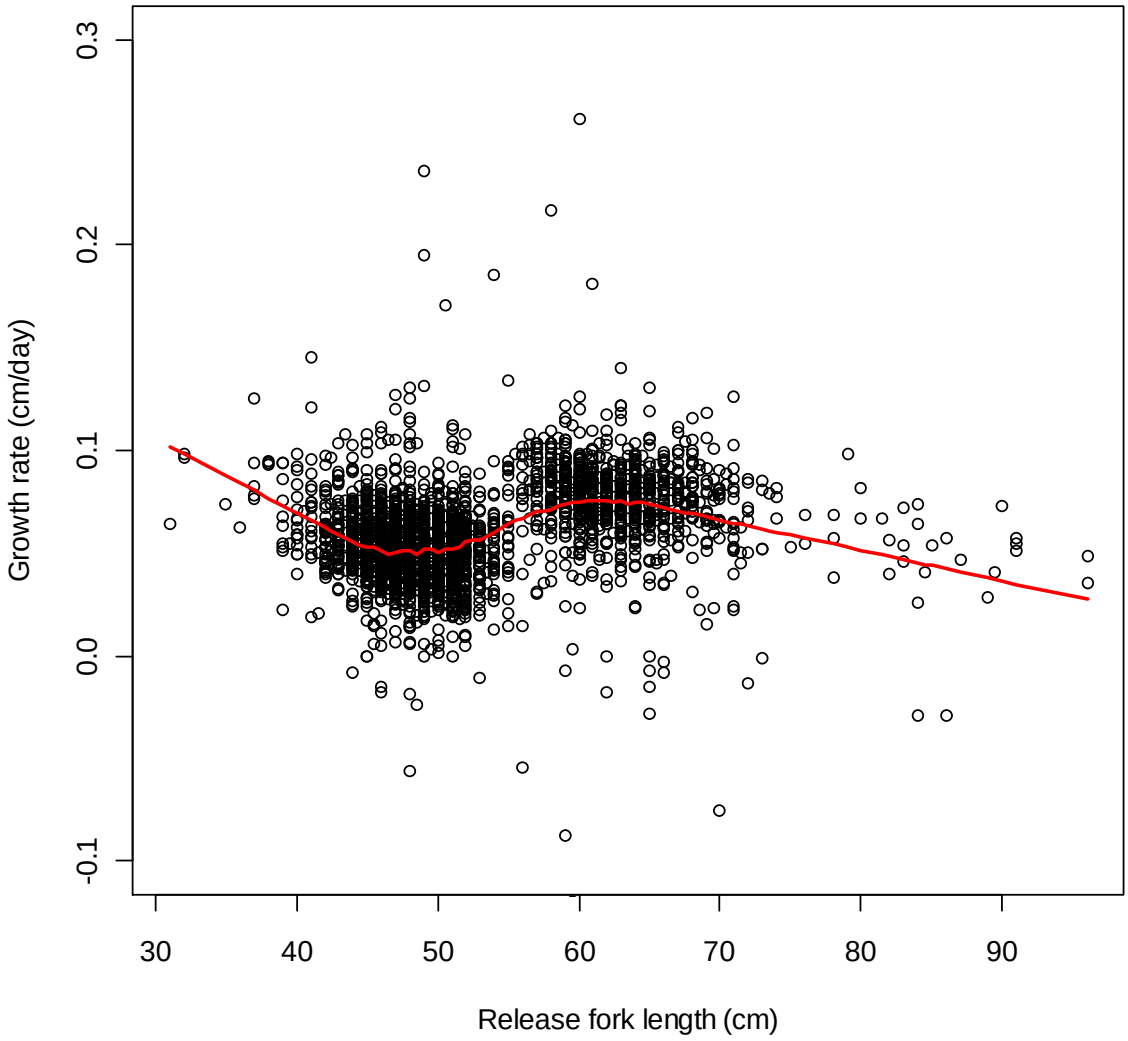

Figure B4 (a-d). Results from fitting a VB log k model jointly to BET tag-recapture and otolith data assuming a log normal distribution for the release ages.

(a) Estimated release age distribution (green line) overlaying conditionally unbiased estimates of individual release ages.

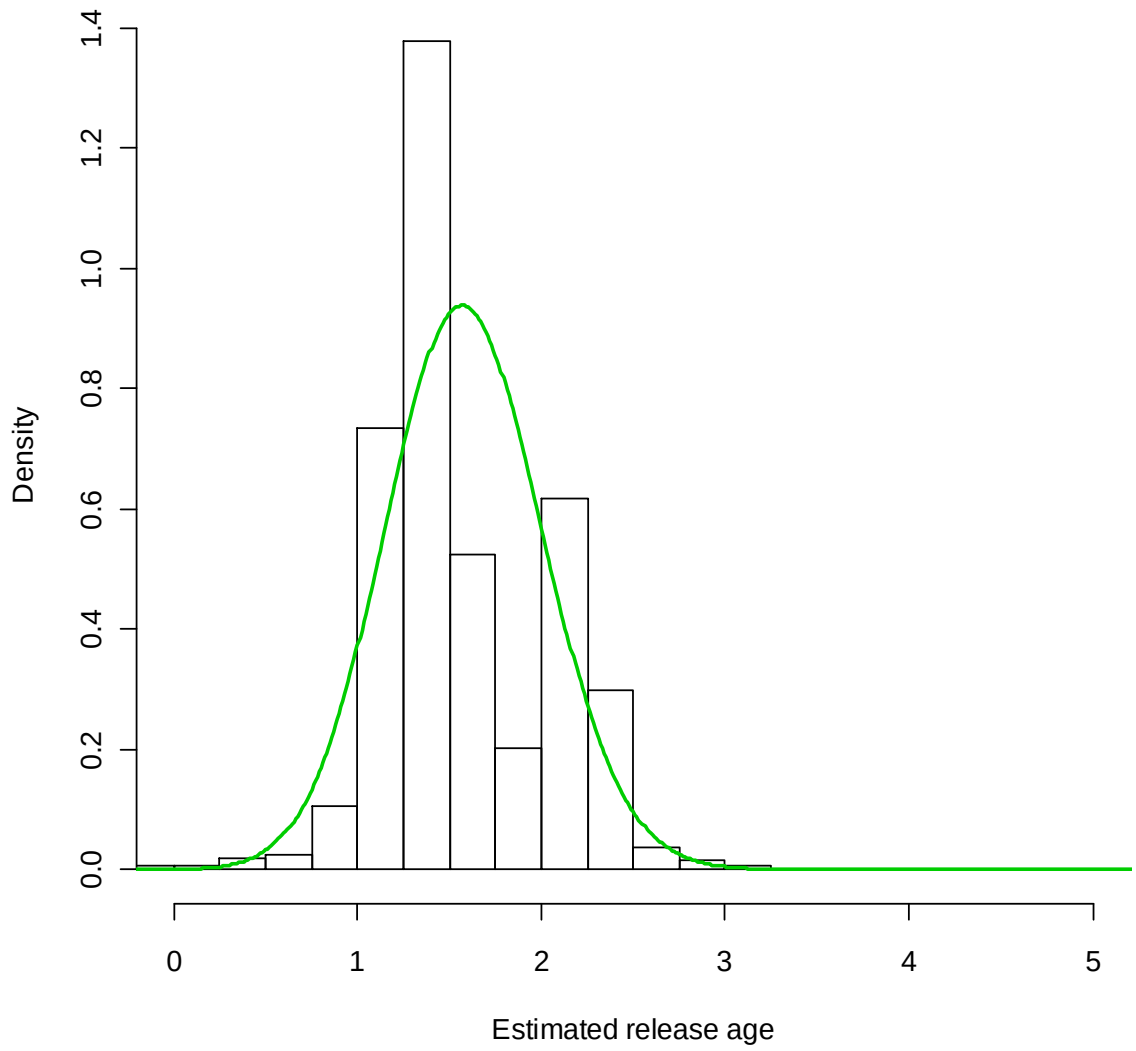

(b) Estimated mean growth curve (black line) and data, Red circles = release points; green triangles=recapture points; blue stars=otolith data. Note that release ages are estimated as in (a), and recapture ages equal estimated release age plus time at liberty. The line segments show fish with negative growth, and explain why some release ages are estimated unrealistically high (so high that they are beyond the limit of the age axis in this case).

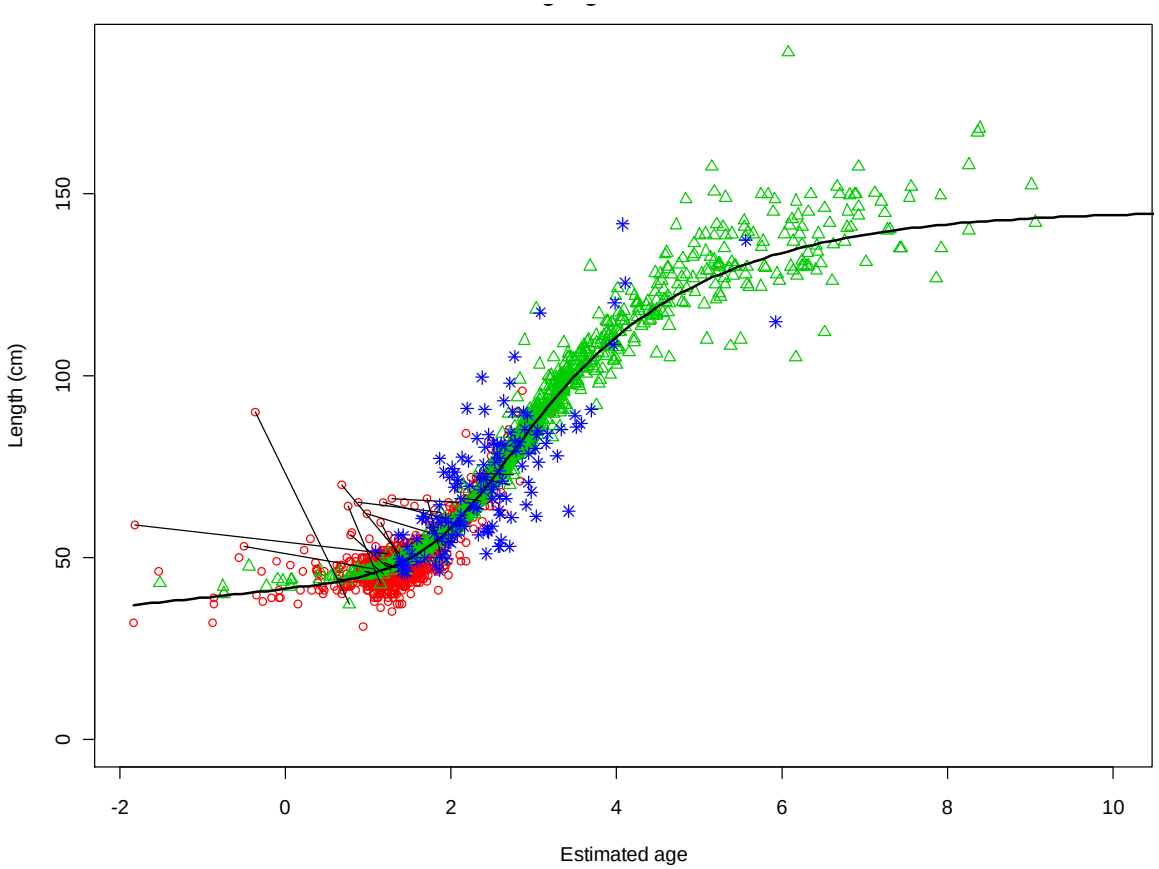

(c) Residuals for tag-recapture data.

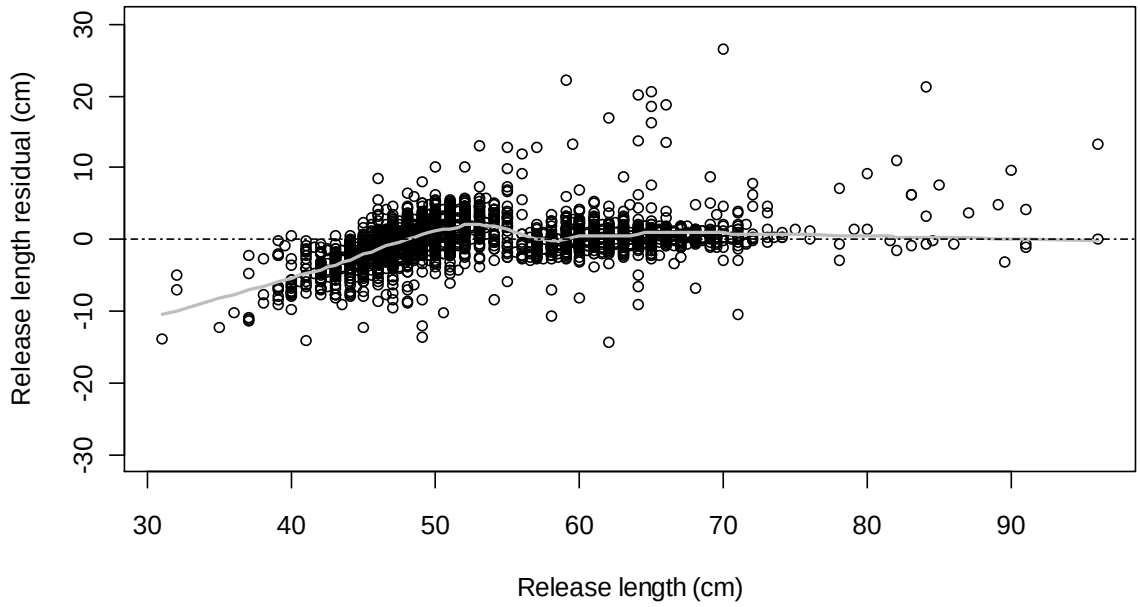

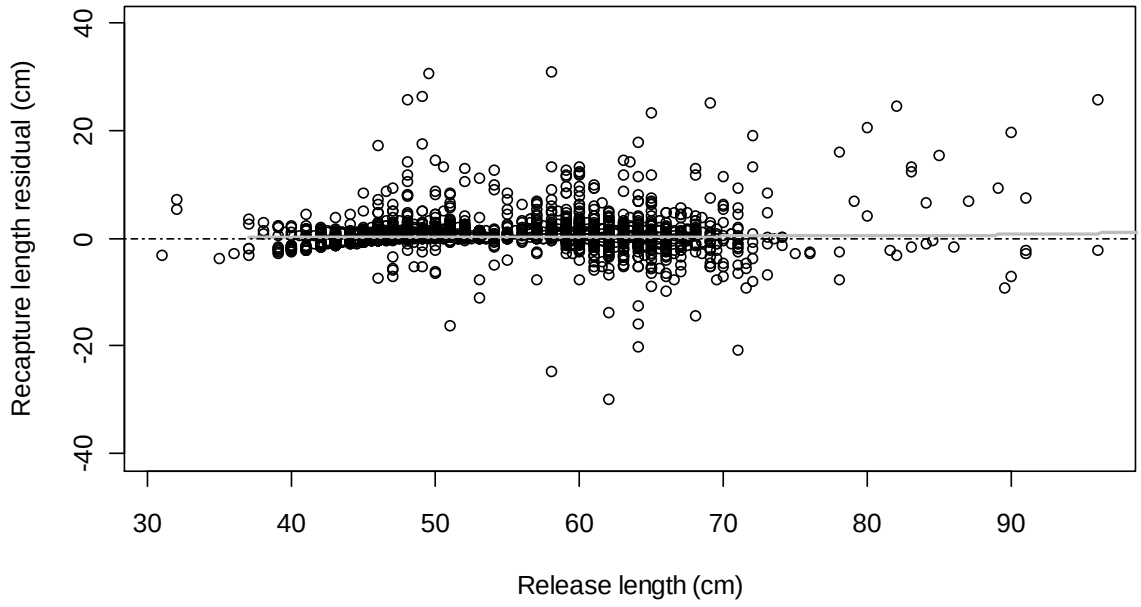

(d) Residuals for otolith data.

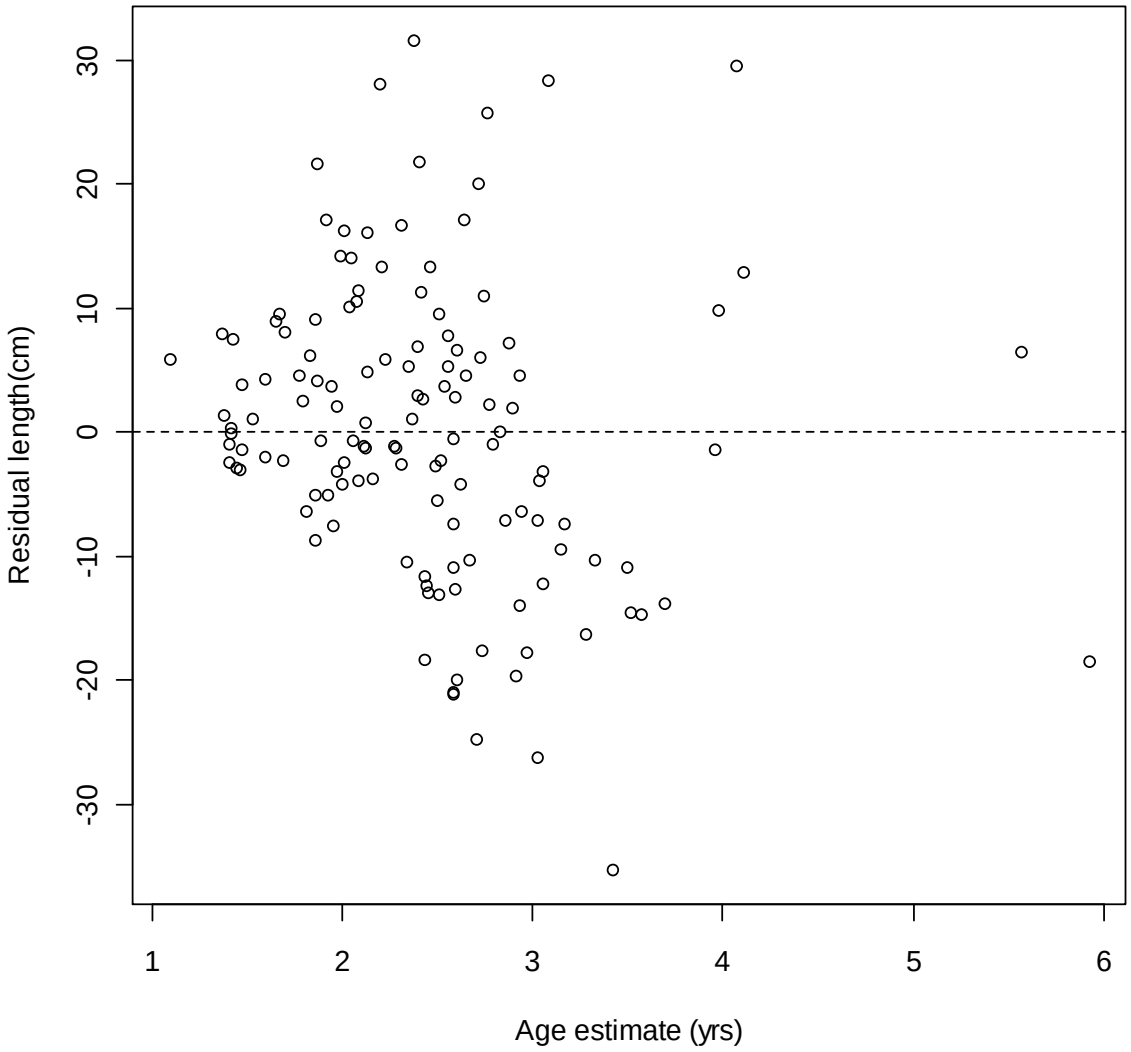

Figure B5 (a-d). Results from fitting a VB log k model jointly to the BET tag-recapture and otolith data assuming a log normal distribution for the release ages, and fixing β at 20 such that the transition between growth stages occurs quickly.

(a) Estimated release age distribution (green line) overlaying conditionally unbiased estimates of individual release ages (β=20).

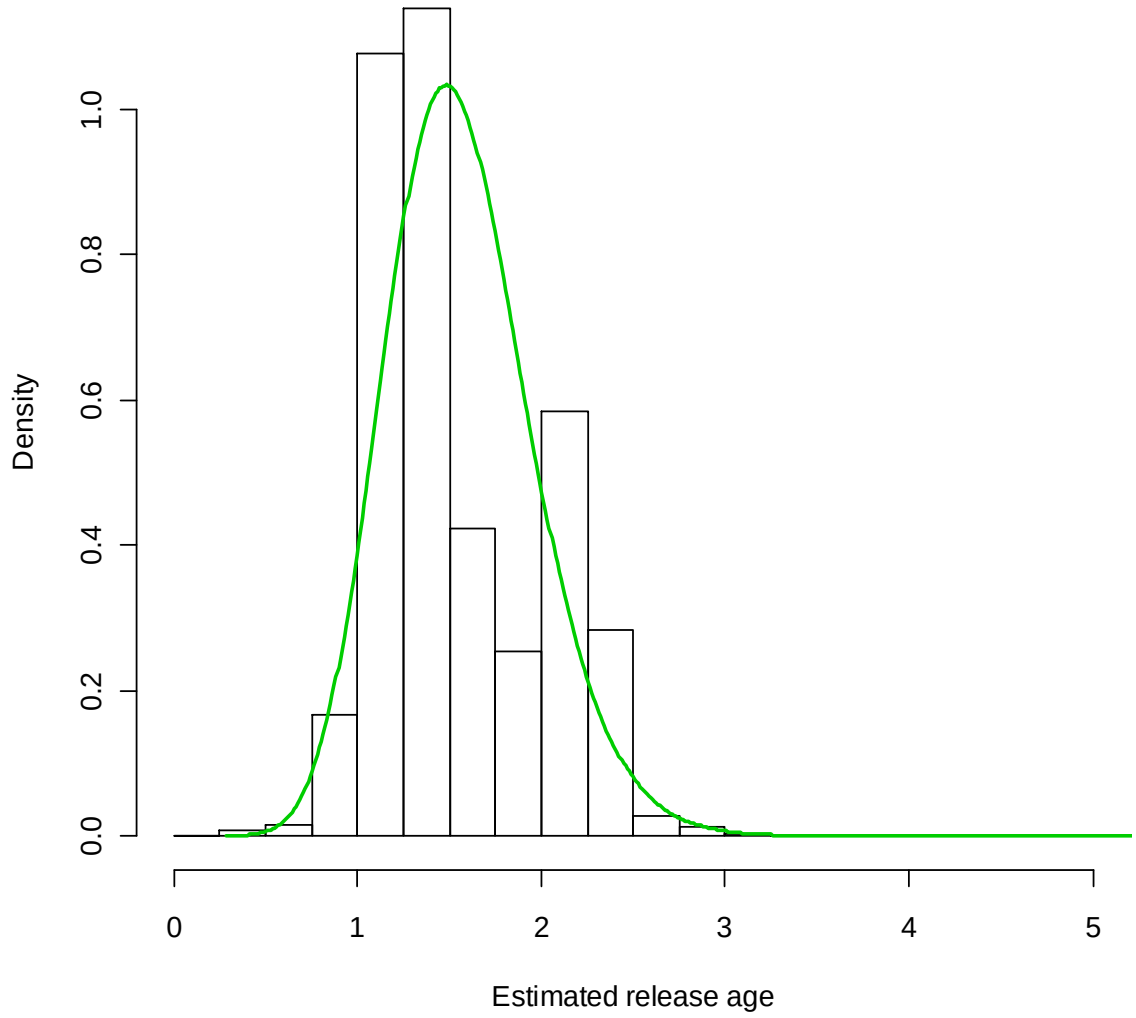

(b) Estimated mean growth curve (black line) and data (β=20). Red circles = release points; green triangles=recapture points; blue stars=otolith data. Note that release ages are estimated as in (a), and recapture ages equal estimated release age plus time at liberty. The line segments show fish with negative growth, and explain why some release ages are estimated unrealistically high.

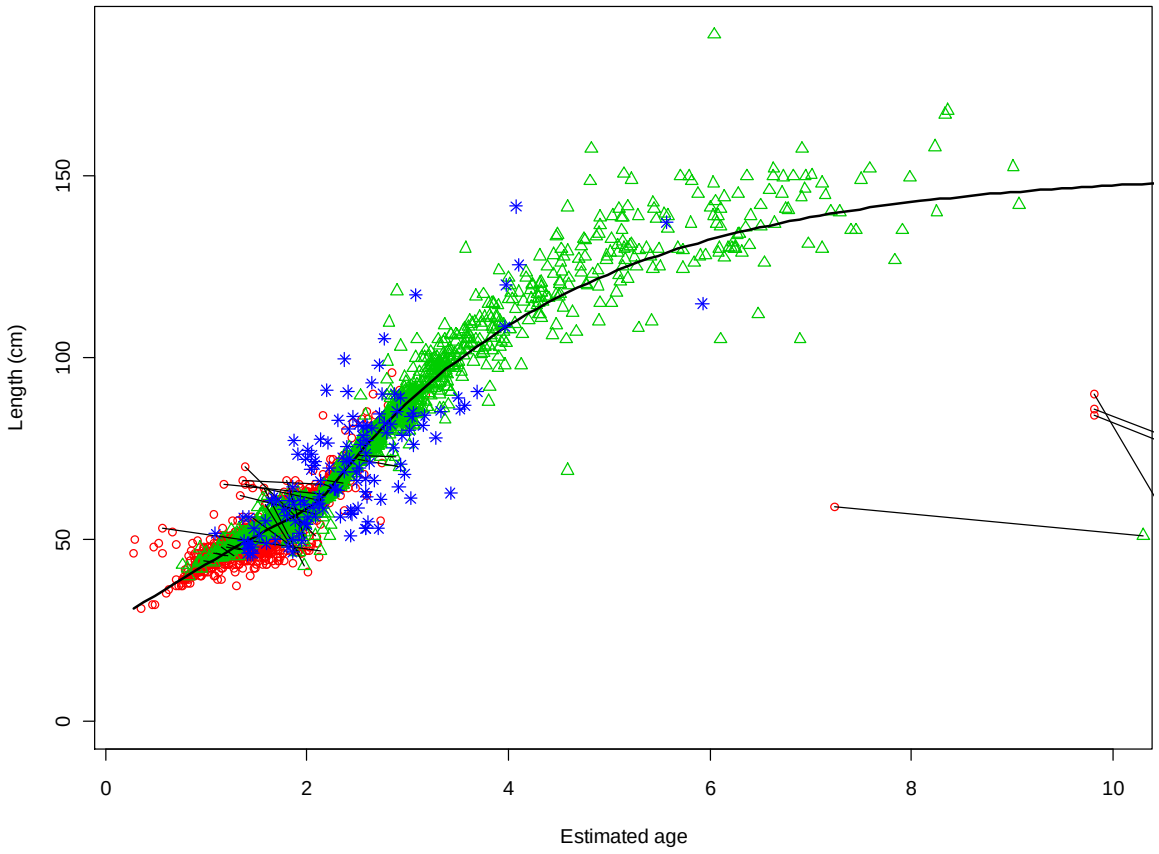

(c) Residuals for tag-recapture data (β=20).

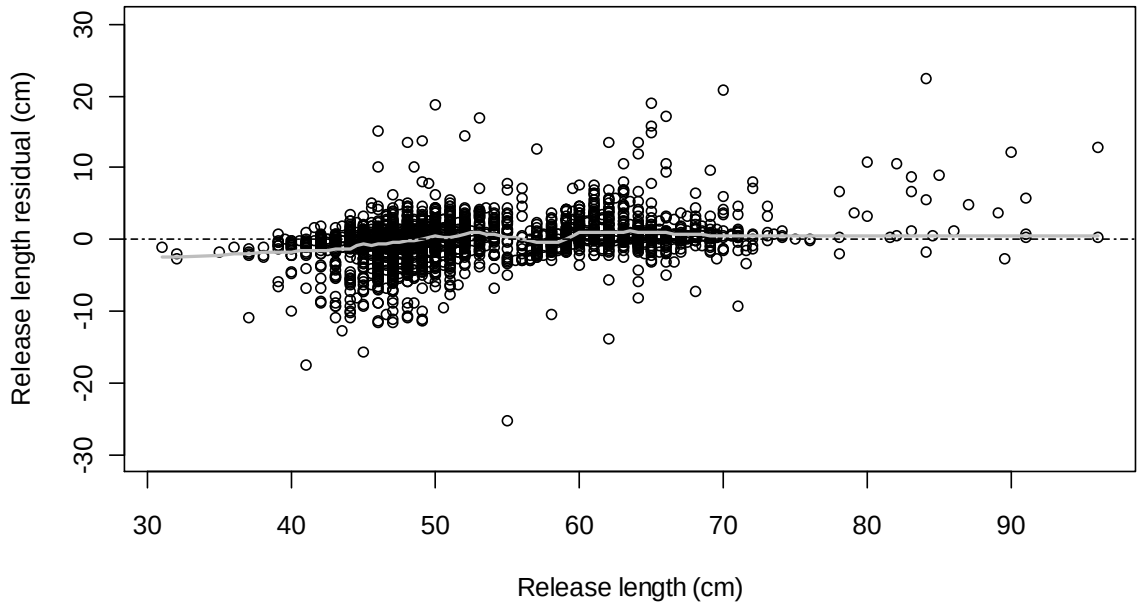

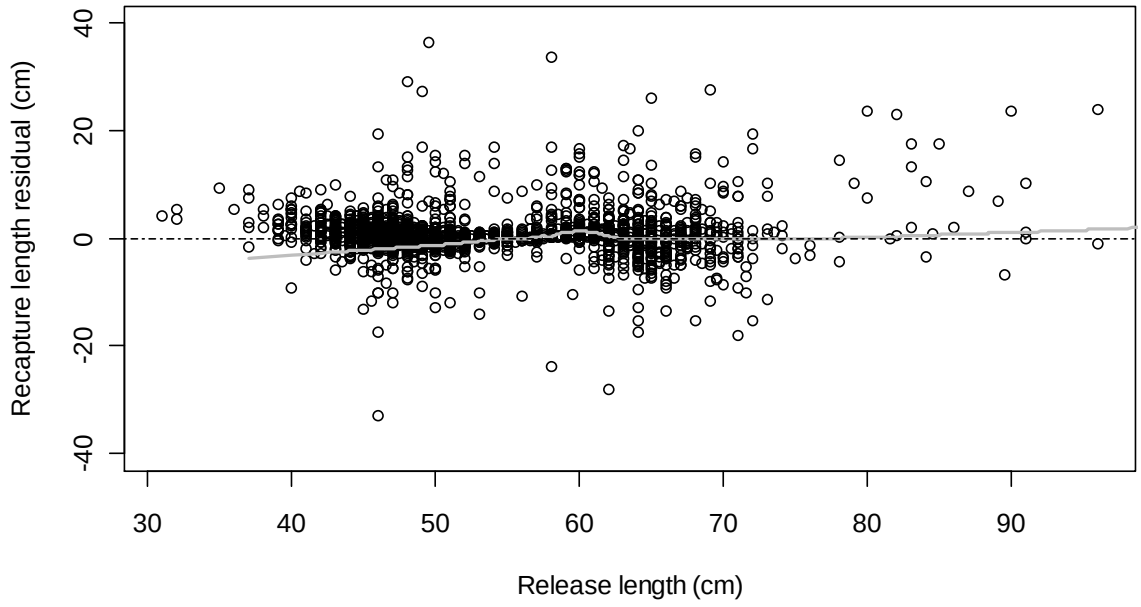

(c) Residuals for otolith data (β=20).

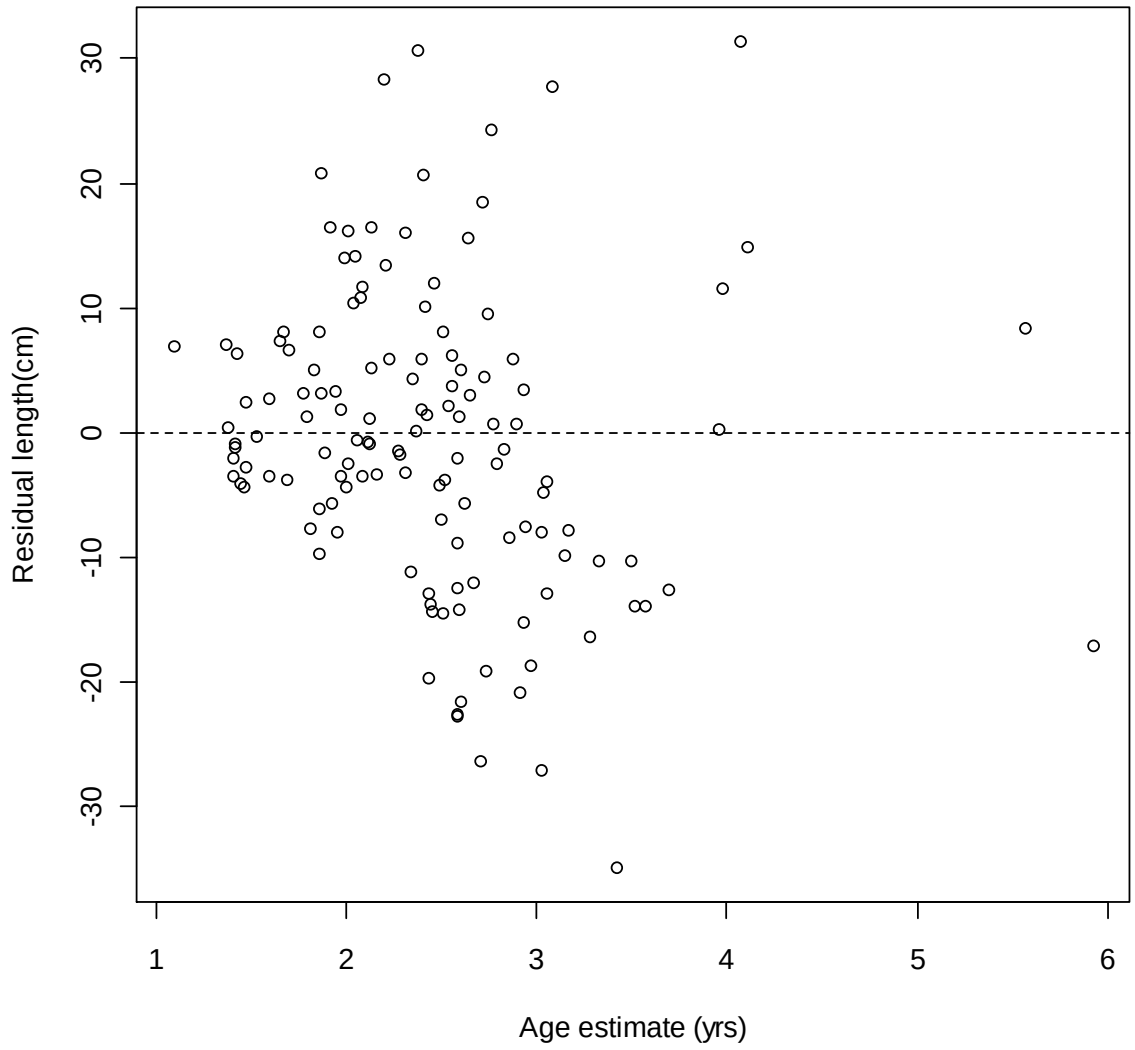

Figure B6. Same as Figure B5(b) except with the release and recapture points for males and females highlighted. To make these points easier to see, the release and recapture data without sex information are shown in black, and the otolith data are omitted.

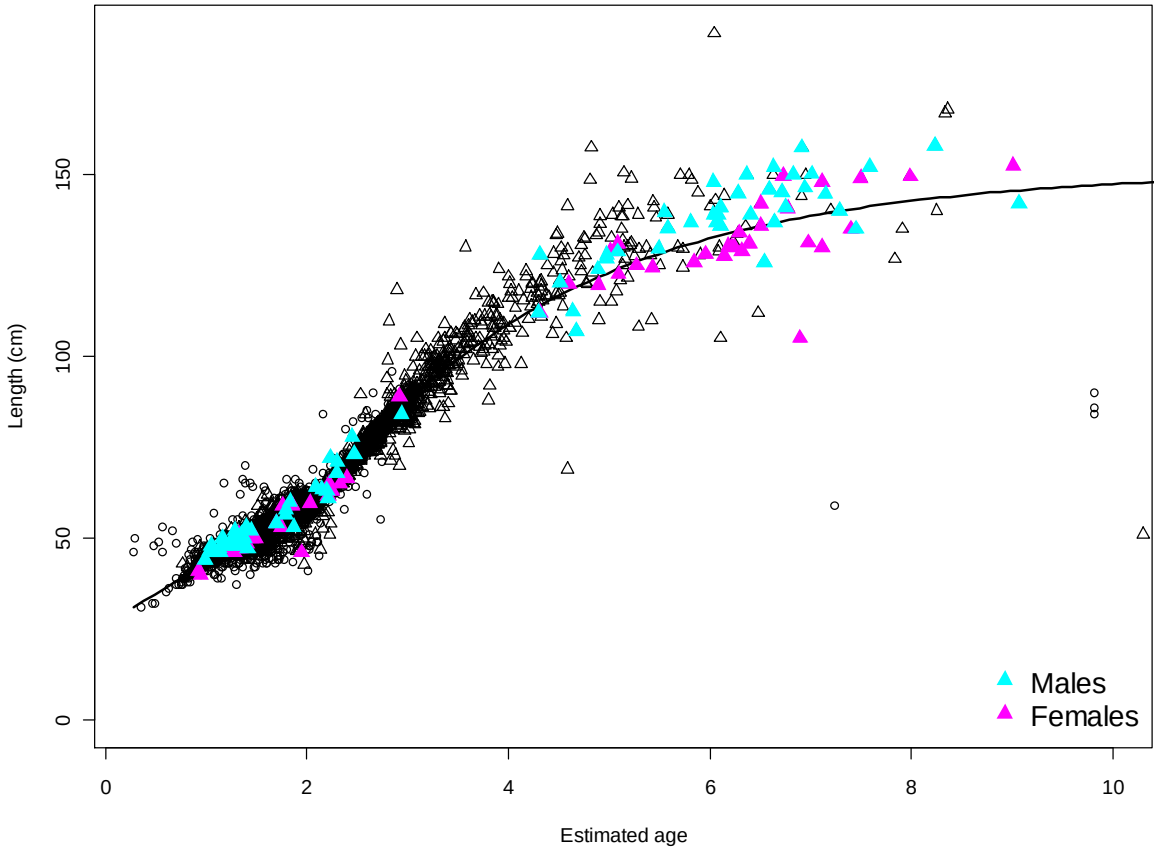

Figure S1. Histograms of (a) release length; (b) recapture length; (c) days at liberty for SKJ.

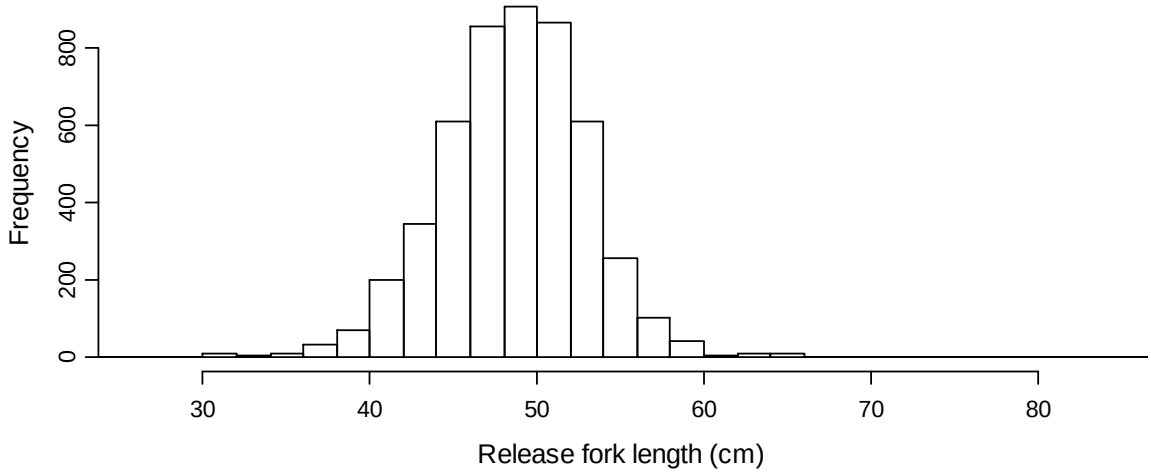

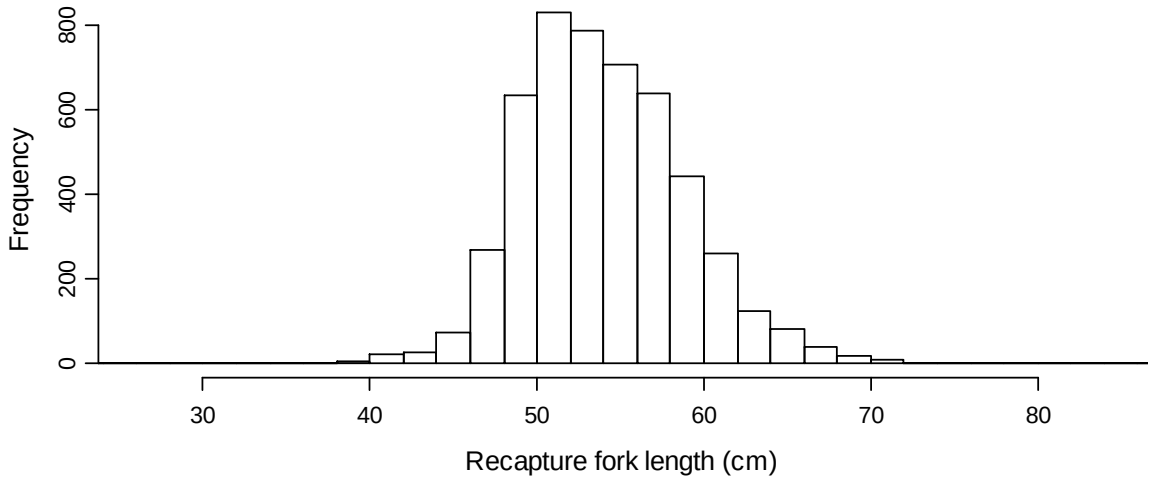

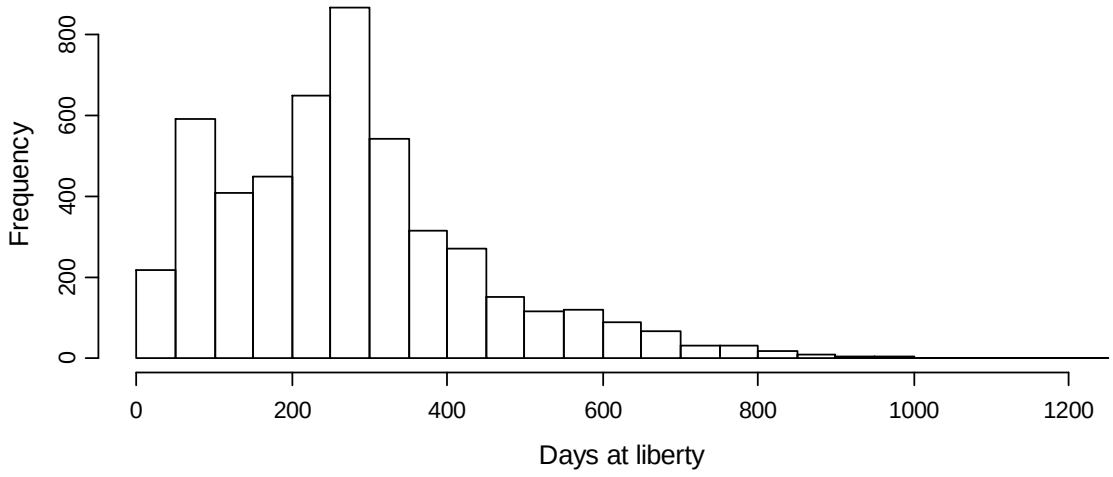

Figure S2. Length increment (recapture length-release length) vs. days at liberty for SKJ.

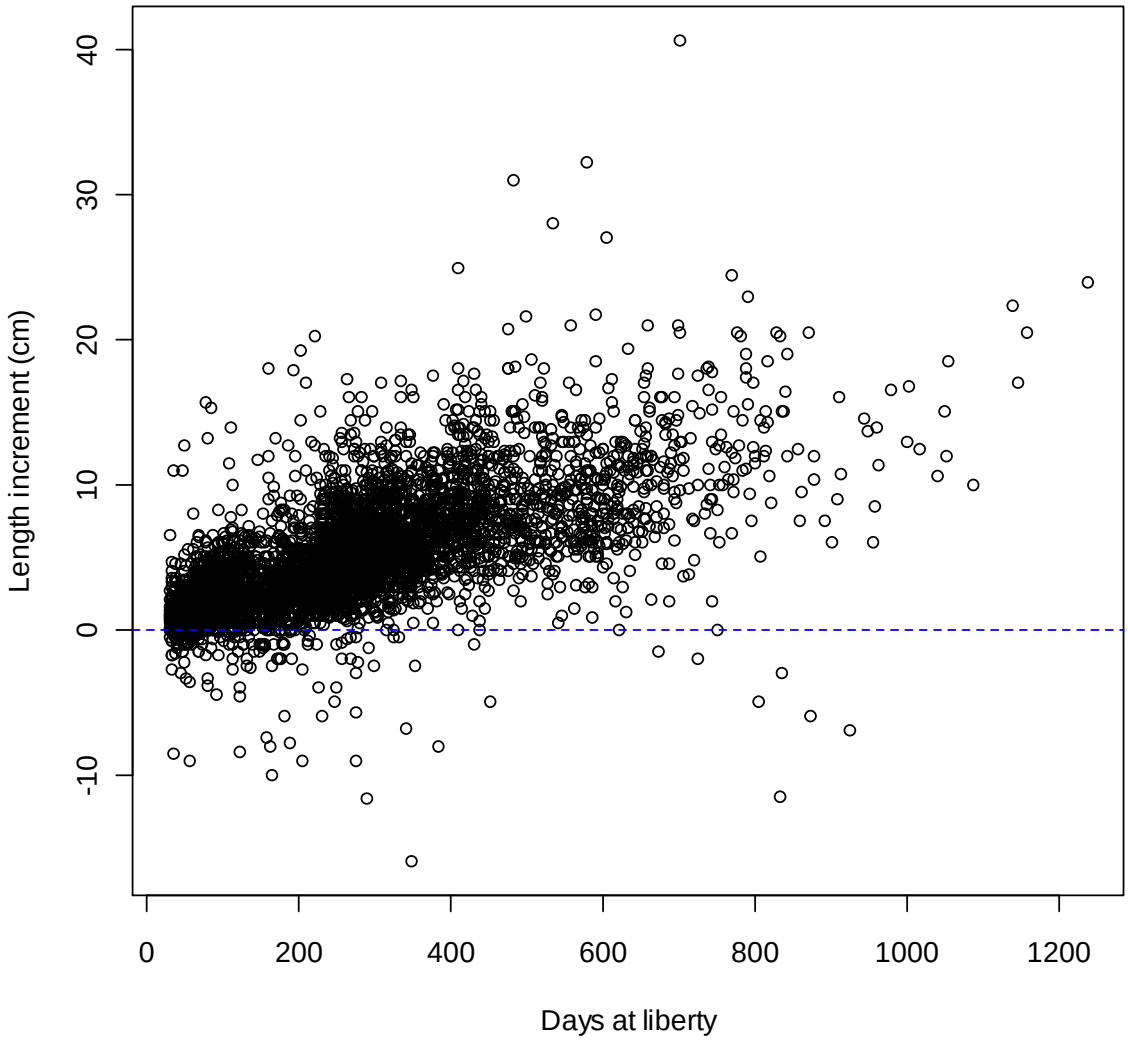

Figure S3. Growth rate vs. release length for SKJ. There is a clear change-point around 45cm, suggesting a 2-stage growth model is more appropriate for SKJ as well.

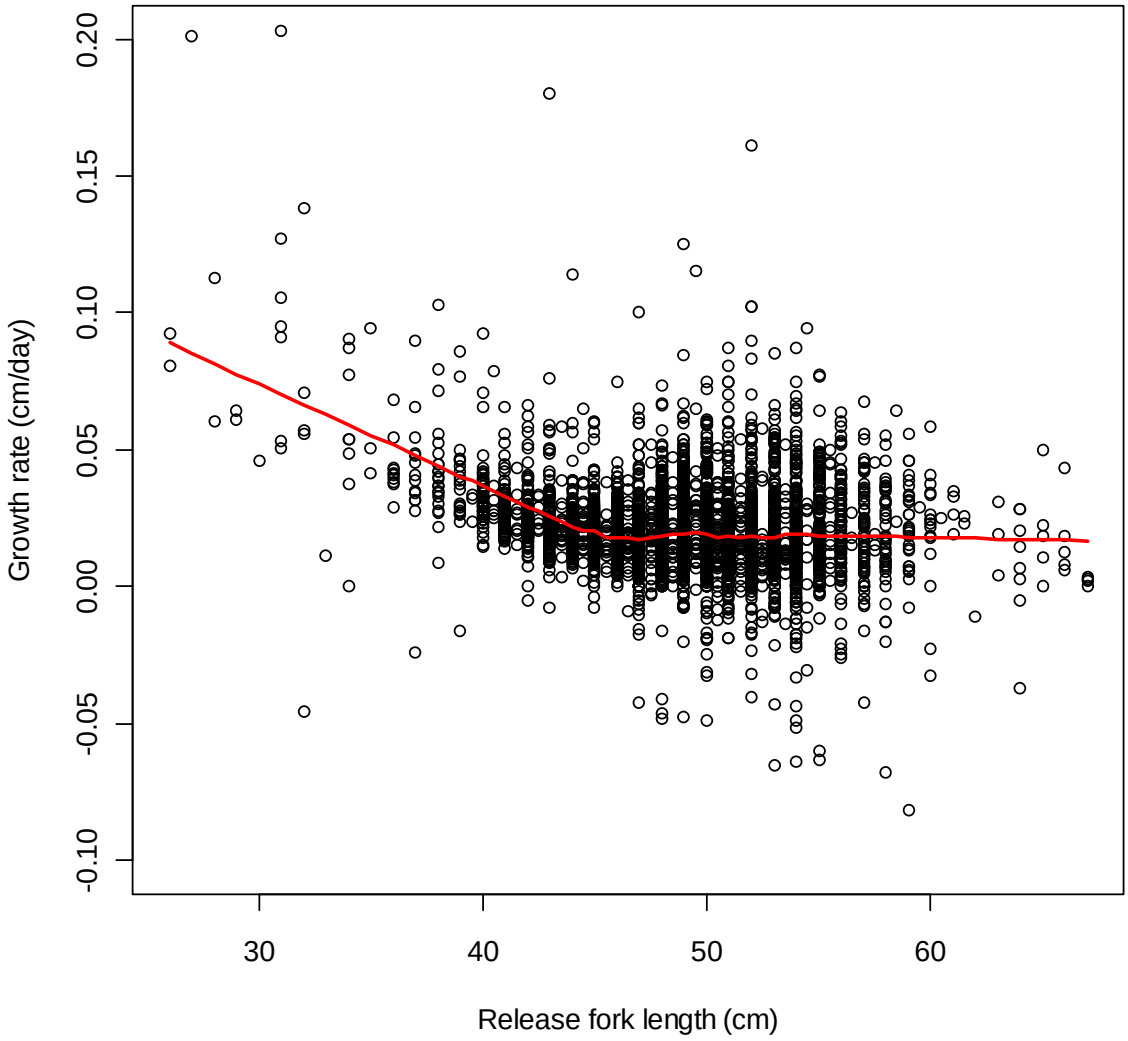

Figure S4 (a-c). Results from fitting a VB log k model to the SKJ tag-recapture data assuming a log normal distribution for the release ages.

(a) Estimated release age distribution (green line) overlaying conditionally unbiased estimates of individual release ages.

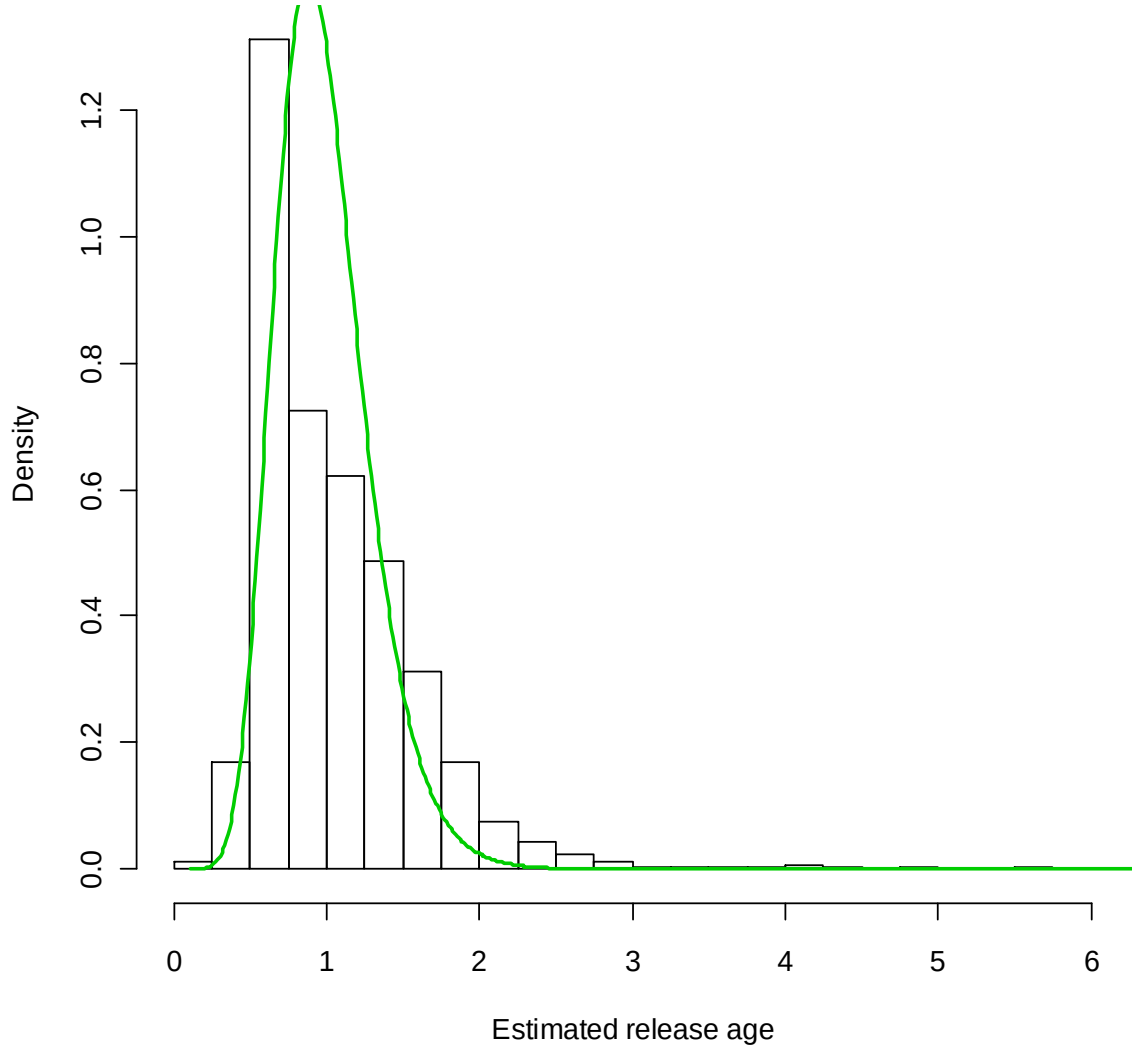

(b) Estimated mean growth curve (black line) and data. Red circles = release points; green triangles=recapture points. Note that release ages are estimated as in (a), and recapture ages equal estimated release age plus time at liberty. The line segments show fish with negative growth, and explain why some release ages are estimated unrealistically high.

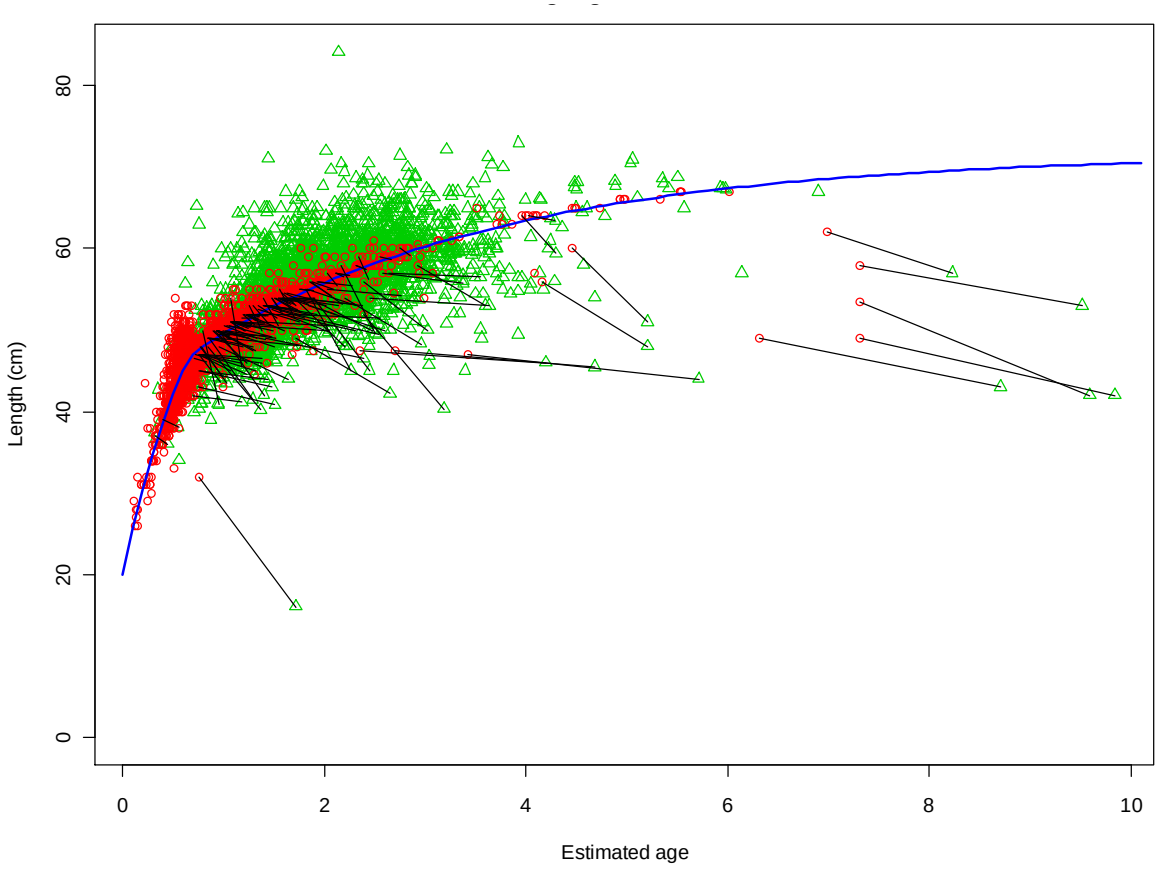

(c) Residuals for tag-recapture data.

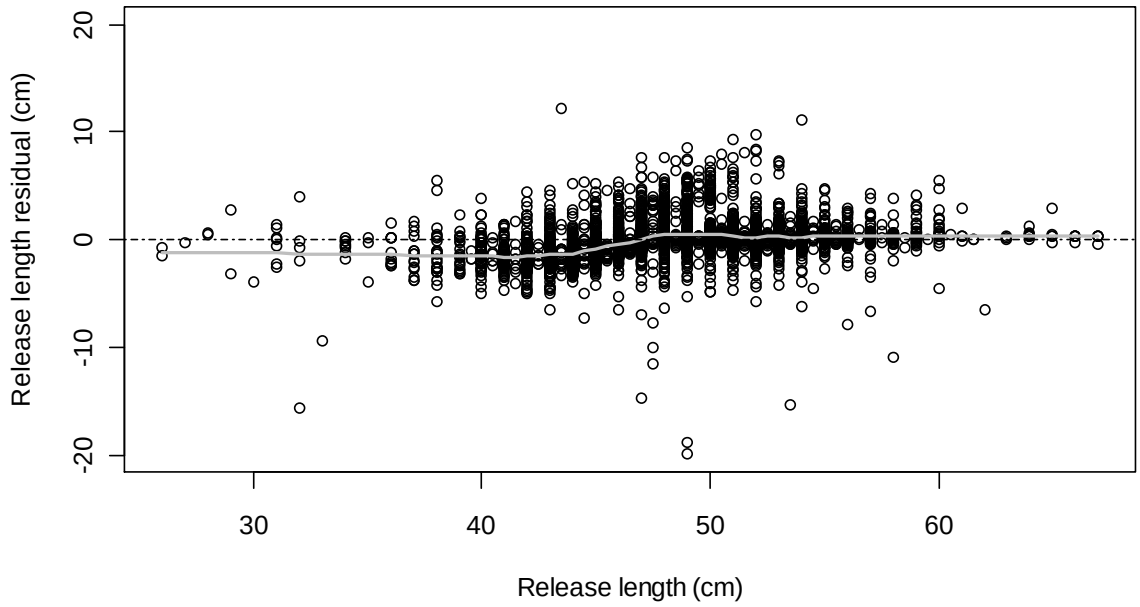

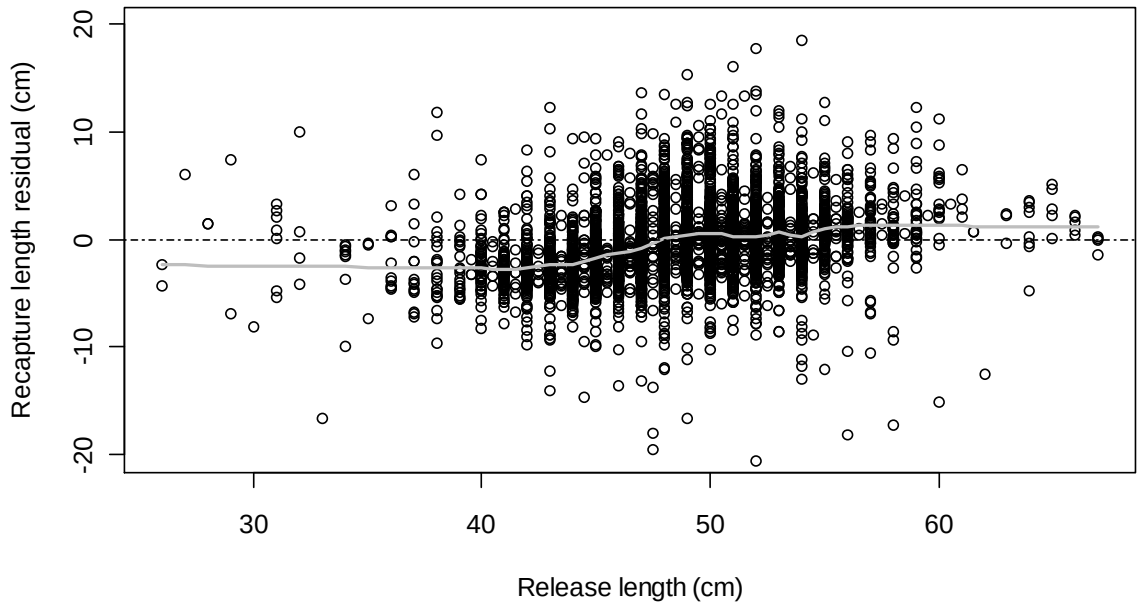

Appendix A. Otolith direct age data

This appendix summarizes data from the otolith readings made at the LEMAR laboratory in France using otoliths collected from YFT, BET and SKJ during the RTTP-IO.

We first concentrate on the readings from otoliths that were OTC-marked at the time of tagging to see how the number of increments counted after the OTC mark (S2) corresponds with number of days the fish was at liberty.

Multiple reads were made by different readers so we first wanted to check for reader effects. An initial investigation comparing S2 counts suggested readers are quite consistent (Figure A1; Table A1). Based on this finding, reader effects were considered insignificant and all of the S2 counts for a given sample were averaged to get a single value for each sample (S2_Mean). A plot of S2_Mean versus days at liberty (Figure A2) shows that the mean S2 counts are very similar to the number of days at liberty for YFT and BET, but much smaller for SKJ. This suggests YFT and BET form daily, or almost daily, increments in their otoliths. The slight underestimate of the counts could be due to biological effects (increments not being formed on a small percent of days) or reader effects (increments not getting counted, perhaps when they are too close together to distinguish). In contrast, SKJ do appear to form daily deposits – note however that Leroy (2000) states that SKJ form daily increments up to ~50cm length, after which this is no longer the case (based on samples collected from the Pacific). The SKJ with S2 counts available for this study were all tagged at lengths >50cm so we could not investigate this hypothesis for the Indian Ocean. As such, only the otolith data for YFT and BET were used in this report for modelling growth.

Linear regressions were fit with S2_Mean as the response variable and days at liberty as the explanatory variable. Models were fit with and without an intercept. The fits without an intercept provided an equally good fit at significance level 0.01, and also appear to fit the lower counts better for YFT and BET (Figure 3). Furthermore, it makes intuitive sense that the S2 counts would be 0 for a fish at liberty 0 days. Thus, the no-intercept models were chosen for adjusting the total increment counts (Stot) to get age estimates. As with the S2 counts, there are multiple Stot counts for each sample (multiple reads per reader and/or multiple readers), so we first averaged them to get a single value for each sample (Stot_Mean). Then, Stot_Mean was divided by the slope of the regression line for the appropriate species (0.93 for YFT; 0.91 for BET) to get an estimate of the fish's age in days.

Age estimates were obtained not only from OTC-marked otoliths, but from any otoliths that had Stot counts available. A summary of the resulting direct age estimates (expressed in years) available for growth modelling is given in Table A2, and plots of fish length versus estimated age for YFT and BET are given in Figure A4. These data were used along with the tag-recapture data as input to the integrated growth models presented in this report.

Epilogue

Subsequent to the above analyses being completed (integrated growth modelling included), correspondence with E. Chassot (also working with the otolith data) led to further investigation of reader effects. It turns out that if a comparison is made between total increment (Stot) counts of different readers, rather than post-OTC (S2) counts, then differences between readers are apparent (Figure A5; Table A3). Reader 1 and Reader 2 still appear to be consistent, but Reader 4 (encompassing all other readers) tends to have lower counts than all other readers; although Reader

4's counts correlate highly with the counts of Readers 1 and 2 (Table A3), suggesting they could possibly be scaled to be consistent with Readers 1 and 2. Reader 3 tends to have lower counts than Readers 1 and 2 and higher counts than Reader 4, but overall his/her counts do not correlate well with any other reader (Table A3).

How best to deal with reader effects in deriving age estimates from the otolith counts is an important issue to be discussed at the upcoming WPTT meeting, because it can have an important influence on the growth model results.

Table A1. Correlation between S2 counts (number of increments after OTC mark) for pairs of readers. Note that Reader 4 corresponds to "Other" in the database, and encompasses reads made by anyone other than Readers 1, 2 and 3.

	Reader 1	Reader 2	Reader 3	Reader 4
Reader 1	1.00	0.97	0.95	1.00
Reader 2		1.00	0.98	0.99
Reader 3			1.00	0.94
Reader 4				1.00

Table A2. Summary of direct age estimates (in years) available for YFT and BET, calculated using methods described in text.

	N	Min	Mean	Max
YFT	236	0.23	2.47	8.36
BET	132	1.09	2.43	5.92

Table A3. Correlation between Stot counts (total number of increments) for pairs of readers. Note that Reader 4 corresponds to "Other" in the database, and encompasses reads made by anyone other than Readers 1, 2 and 3.

	Reader 1	Reader 2	Reader 3	Reader 4
Reader 1	1.00	0.90	0.40	0.90
Reader 2		1.00	0.53	0.90
Reader 3			1.00	0.52
Reader 4				1.00

Figure A1. Compare S2 counts (number of increments after OTC mark) between readers. If a reader made multiple reads on a given otolith, these were averaged. Note that Reader 4 corresponds to "Other" in the database, and encompasses reads made by anyone other than Readers 1, 2 and 3.

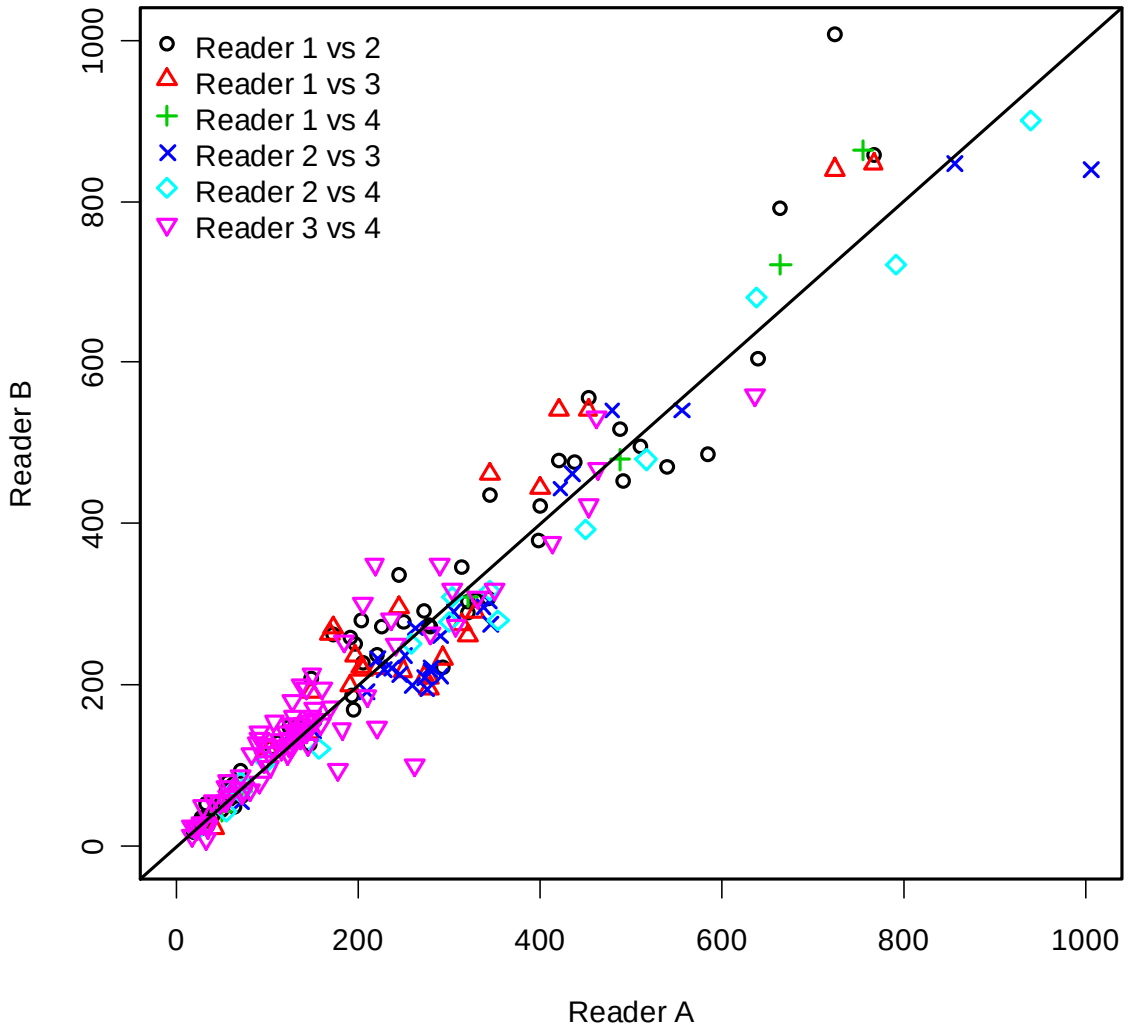

Figure A2. Number of increments counted after the OTC mark averaged over all reads (S2_Mean) versus time at liberty (TAL) in days. Only samples for which the CV of all reads was less than 0.1 are plotted. The 1:1 line is shown in black.

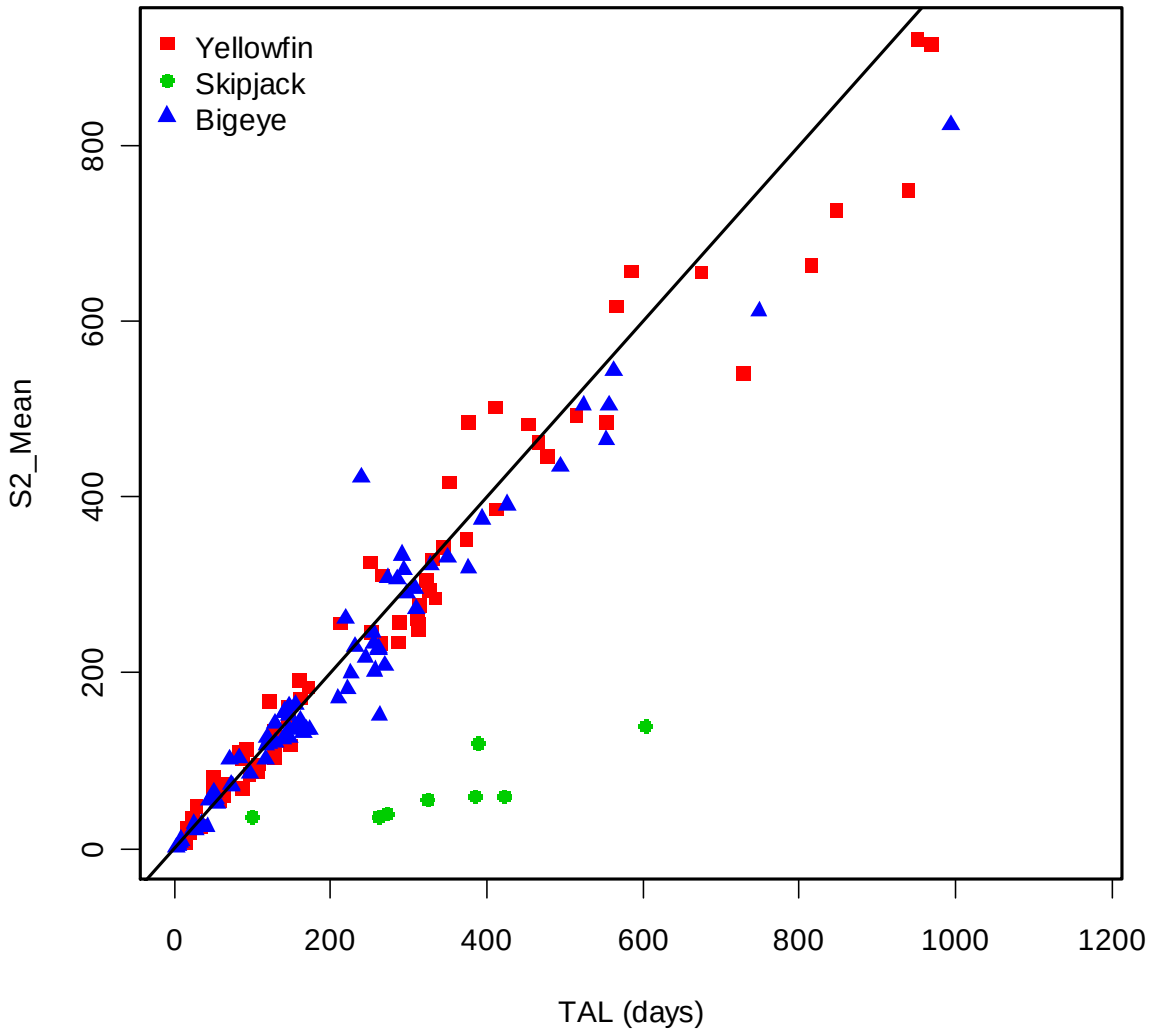

Figure A3. Linear regression fits of mean number of increments counted after the OTC mark (S2_Mean) versus time at liberty (TAL) in days for (a) yellowfin and (b) bigeye. Models with and without an intercept are compared. Only samples for which the CV of all reads was less than 0.1 were used in the regressions.

(a) Yellowfin

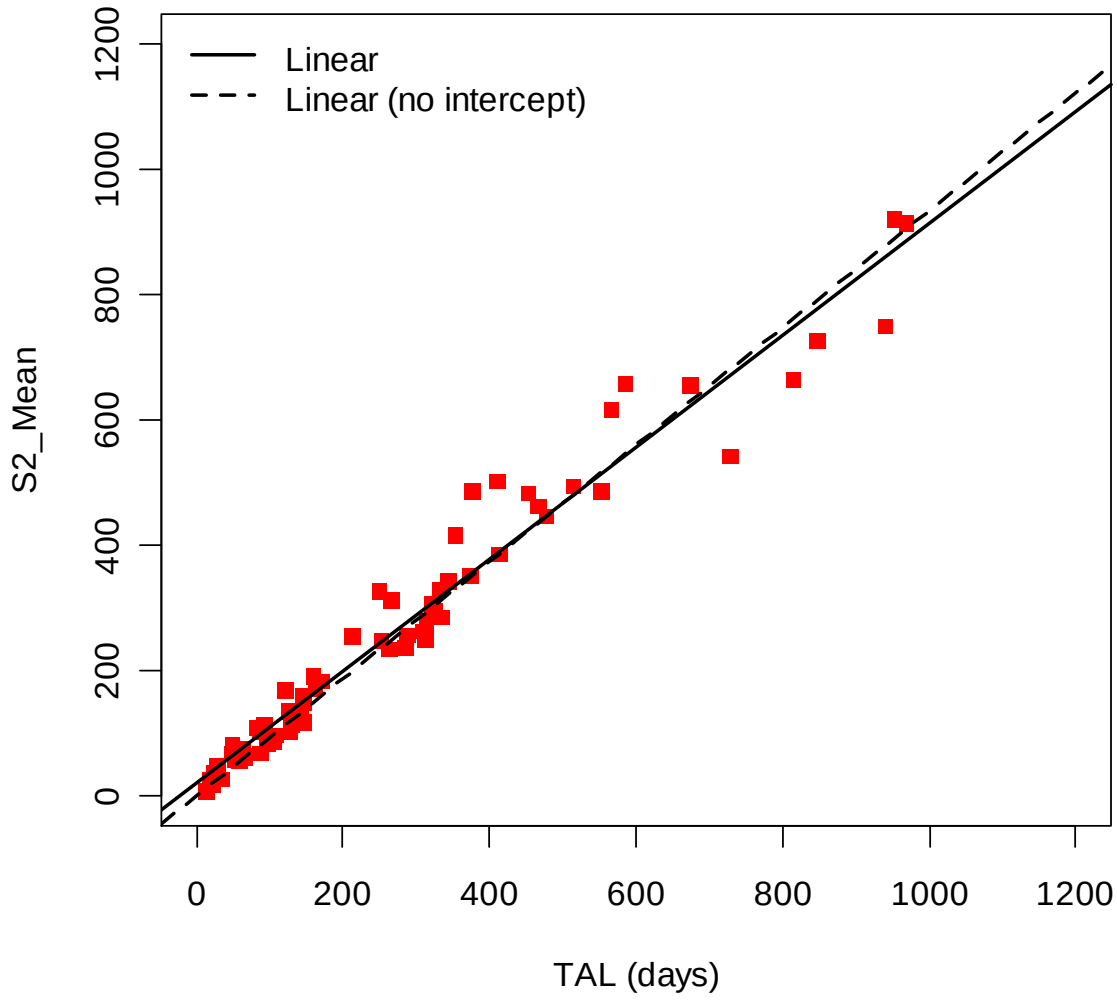

(b) Bigeye

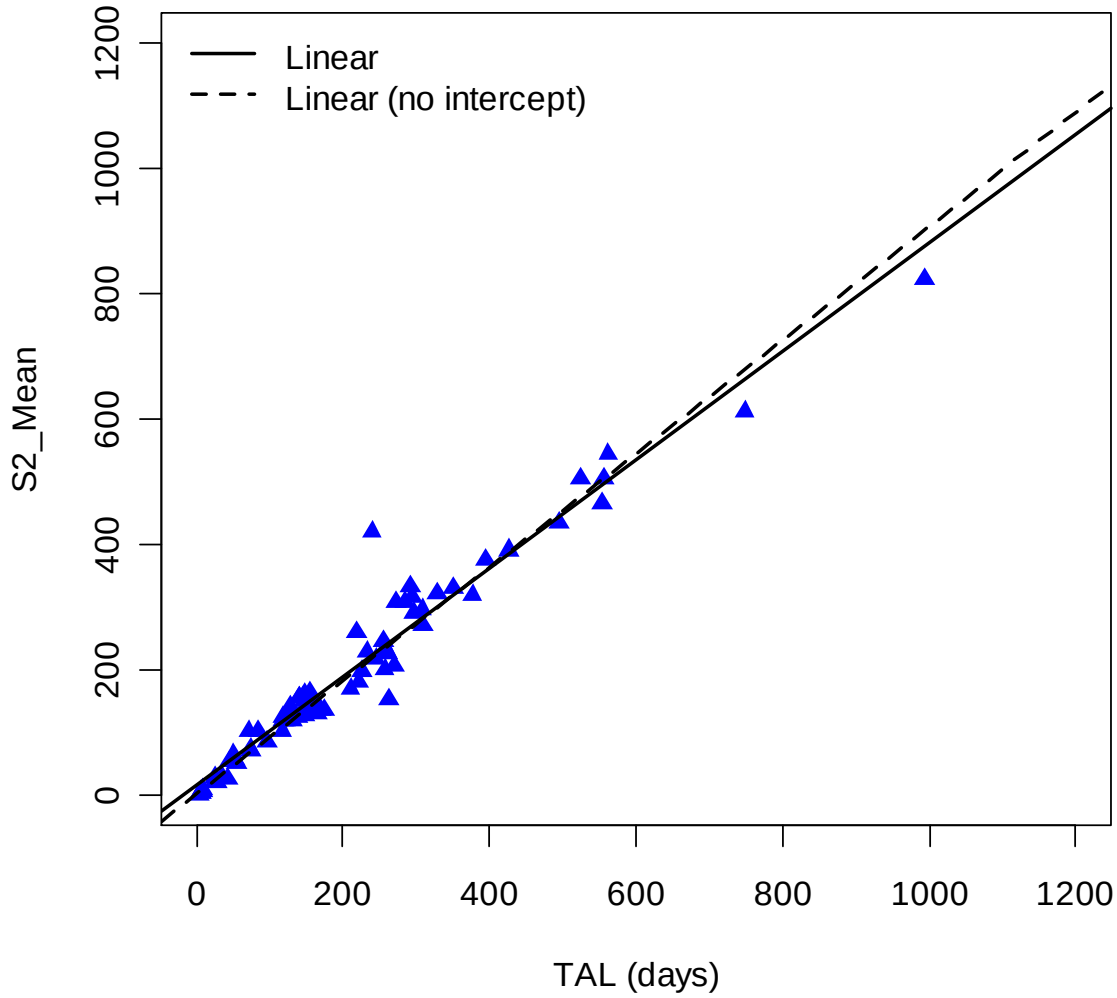
Linear
Linear (no intercept)
S2_Mean
TAL (days)
0
200
400
600
800
1000
1200

Figure A4. Fish length (cm) versus estimated age (yrs) for (a) yellowfin and (b) bigeye. Error bars indicate +/- 1 standard error for the age estimate. Standard errors were calculated using the variance of the multiple reads for a given otolith (they do not take into account uncertainty in the linear regression slope used to adjust the reads).

(a) Yellowfin

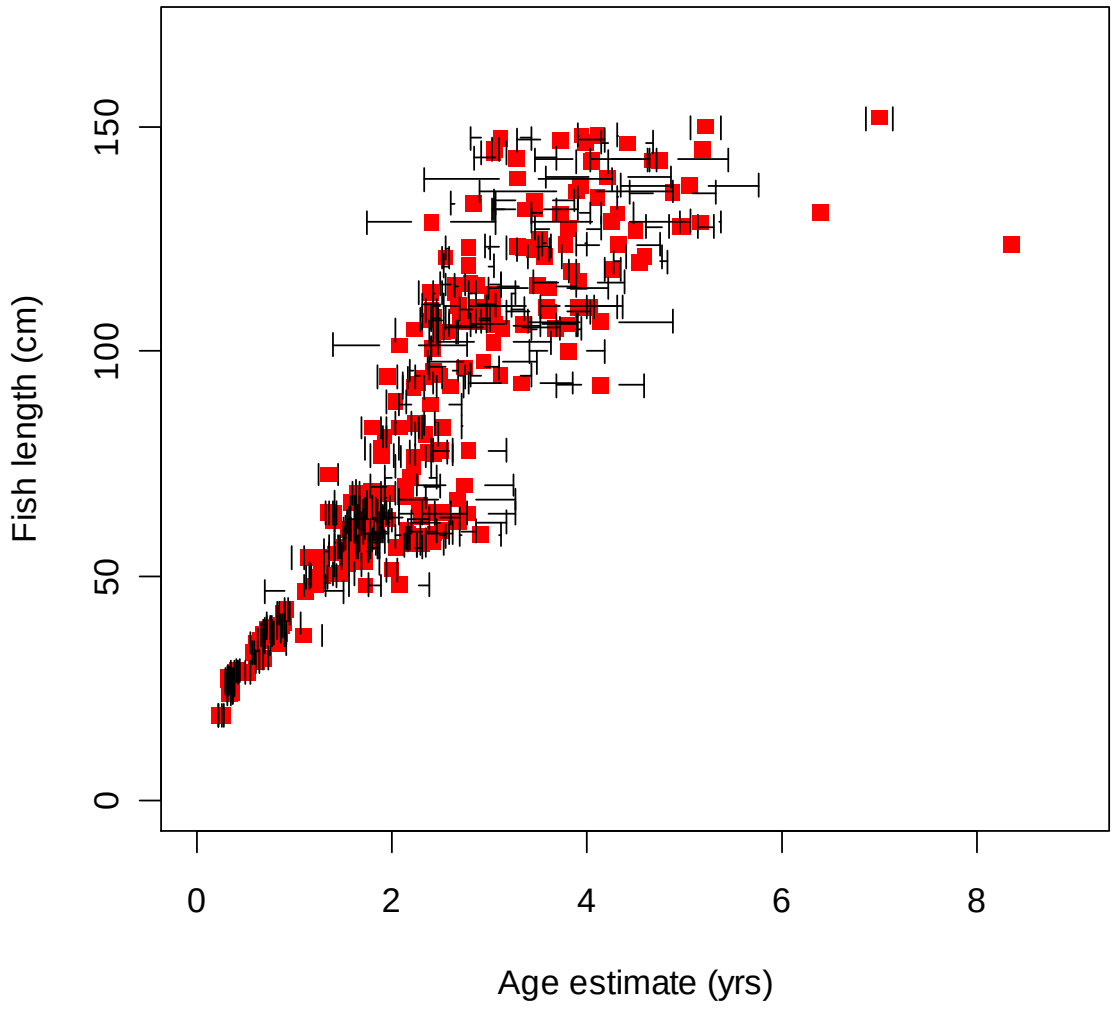

(b) Bigeye

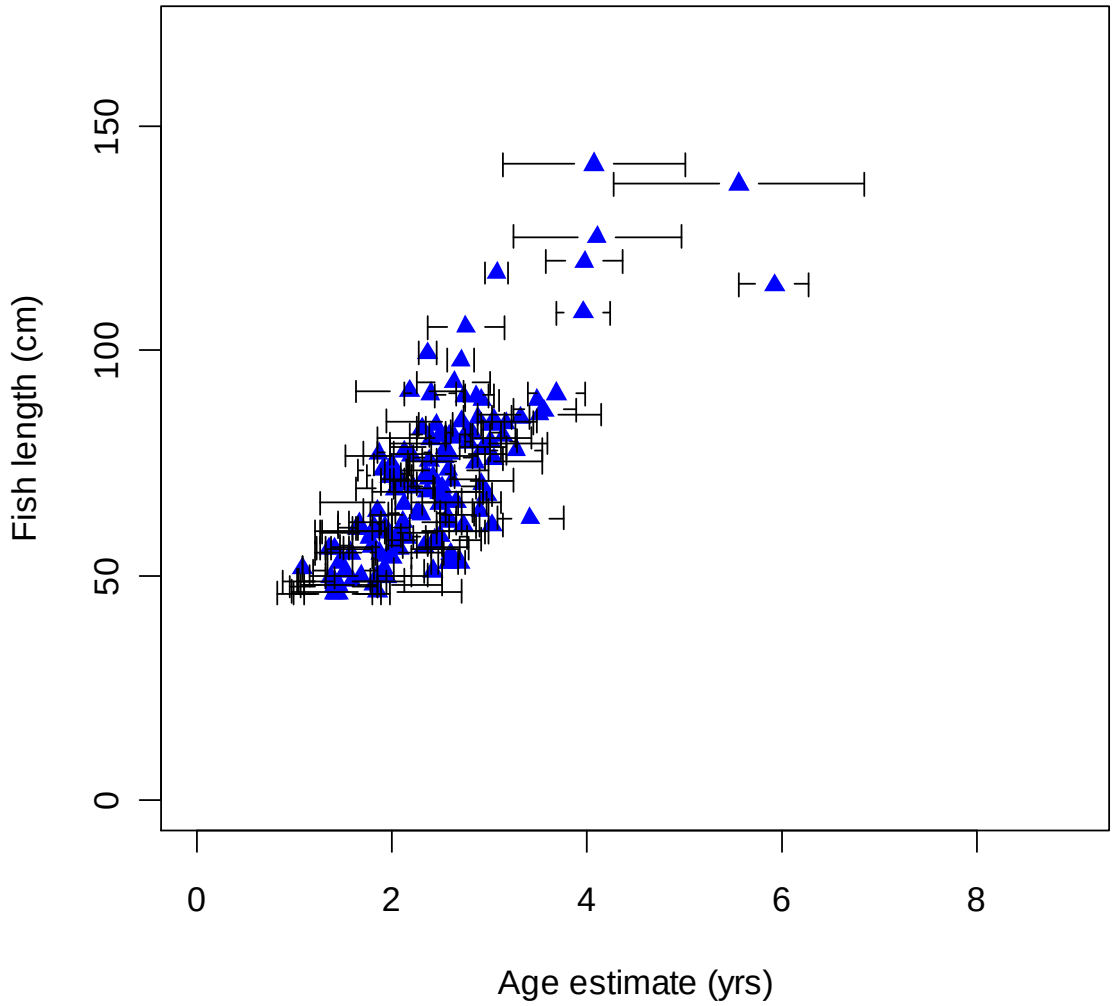

Figure A5. Compare Stot counts (total number of increments) between readers. If a reader made multiple reads on a given otolith, these were averaged. Note that Reader 4 corresponds to "Other" in the database, and encompasses reads made by anyone other than Readers 1, 2 and 3.